

Book Chapter 1, “Energy Conversion & Green Energy Storage”, Editors (A. Soni, D. Tripathi, J. Sahariya, and K. N. Sharma), CRC Press, Boca Raton, Florida, USA (2022).

Accepted July 30th 2022

COMPUTATIONAL FLUID DYNAMIC SIMULATION OF THERMAL CONVECTION IN GREEN FUEL CELLS WITH FINITE VOLUME AND LATTICE BOLTZMANN METHODS

O. Anwar Bég^A, Hamza Javaid^B, T. A. Bég^C, V.R. Prasad^D, S. Kuharat^E, Ali Kadir^F,

H. J. Leonard^A, W.S. Jouri^A, Z. Ozturk^E and Umar F. Khan^F

^A*Multi-Physical Engineering Sciences Group (MPESG), Department of Mechanical and Aeronautical Engineering, School of Science, Engineering and Environment (SEE), Newton Building, Salford University, Manchester, M54WT, UK.*

^B*Mechanical Engineer, Automotive Financial Services, Manchester, UK.*

^C*Engineering Mechanics Research, Israfil House, Dickenson Rd., Manchester, M13, UK.*

^D*Department of Mathematics, School of Advanced Sciences, Vellore Institute of Technology, Vellore– 6322014, India.*

^E*Research Fellow-Energy Modelling, Think Lab, Maxwell Building, University of Salford, Manchester, M5WT, UK.*

^F*Electromagnetics and Fuel Cell Research, School of Engineering, Robert Gordon University, Aberdeen, Scotland.*

***Corresponding author, Director-MPESG and Professor of Engineering Science; Email: O.A.Beg@salford.ac.uk**

ABSTRACT

The modern thrust for green energy technologies has witnessed considerable efforts in developing efficient, environmentally friendly fuel cells. This has been particularly so in the automotive sector which is the dominant mode of personal transport in the 21st century. Toyota has led this fuel revolution and has already implemented a number of hybrid vehicles commercially. PEM (Proton-exchange membrane fuel cells, also known as polymer electrolyte membrane), AFC (alkaline) and PAFC (phosphoric acid) and SOFC (solid oxide fuel cells) using Hydrogen/Oxygen, in particular, have demonstrated significant popularity. Such fuel cells have several distinct advantages include reduced emissions (generally water vapour and some heat) and an absence of moving parts requiring significantly less maintenance than conventional internal combustion engines. Salford university has established a major vision for “smart living” and eco-friendly hydrogen fuel cells exemplify this approach. Motivated by this, in the present work a detailed computational fluid dynamic simulation of simplified fuel cell systems are presented. ANSYS FLUENT finite volume commercial software (version 19) has been deployed to simulate flow characteristics and temperature distributions in a 2-dimensional enclosure replicating a hybrid hydrogen-oxygen fuel cell of the PEM, AFC/PAFC and SOFC type. This work has been conducted as a final year undergraduate project in mechanical engineering (by the second author), supervised by the first author. Further input from co-authors has refined the simulations and identified important physical implications for the next generation of hydrogen-oxygen fuel cells. Extensive visualization of transport phenomena in the fuel cell is included i.e. streamline and isotherm contours. Validation of the finite volume computations has also been achieved with a thermal Lattice Boltzmann method (LBM) achieving excellent agreement. Mesh independence tests are also performed. The simulations constitute a first step and are being extended to consider three-dimensional transient circulation flows in hydrogen fuel cells.

KEY WORDS: PEM, AFC/PAFC, SOFC (Hydrogen/oxygen) fuel cells; heat transfer; computational fluid dynamics; automotive engineering; green technology; isotherms; circulation zones; vortex cells; mesh generation; ANSYS FLUENT; thermal Lattice Boltzmann method (LBM).

1.INTRODUCTION

A fuel cell is a device that converts chemical potential energy (energy stored in molecular bonds) into electrical energy. A PEM (Proton Exchange Membrane) cell uses hydrogen gas (H₂) and oxygen gas (O₂) as fuel. The products of the reaction in the cell are water, electricity, and heat. This is a substantial Improvement over internal combustion engines, coal burning power plants, and nuclear power plants, all of which produce harmful by-products. Since O₂ is readily available in the atmosphere, it is merely required to supply the fuel cell with H₂ which can come from an electrolysis process [1]. Many advantages are achieved with PEM fuel cells. By converting chemical potential energy directly into electrical energy, fuel cells avoid the “thermal

bottleneck" (a consequence of the 2nd law of thermodynamics) and are thus inherently more efficient than combustion engines, which must first convert chemical potential energy into heat, and then mechanical work. Also, direct emissions from a fuel cell vehicle are just water and a little heat. This is a marked improvement over the internal combustion engine's litany of greenhouse gases. Fuel cells have no moving parts. They are thus much more reliable than traditional engines and circumvent the need for continuous maintenance and diagnostics [2]. An example of the mechanism of a PEM fuel cell is shown in Fig. 1.

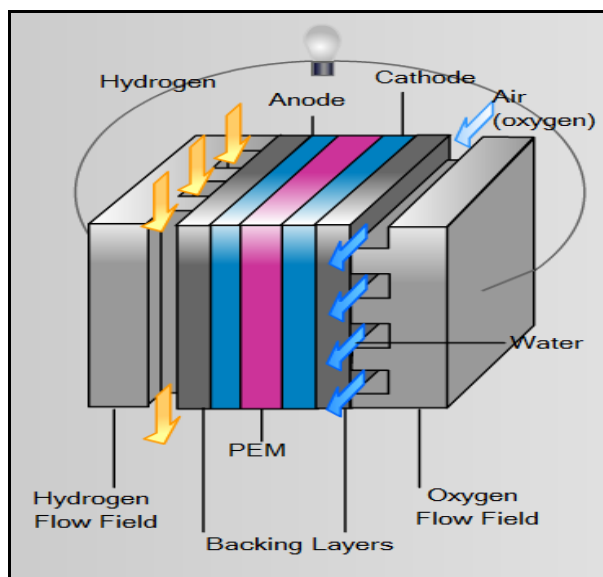


Fig 1: Modern PEM fuel cell design [Cathode: $O_2 + 4H^+ + 4e^- \rightarrow 2H_2O$, Anode: $2H_2 \rightarrow 4H^+ + 4e^-$
Overall: $2H_2 + O_2 \rightarrow 2H_2O$] [Stanford University-reproduced with permission]

There are four fundamental components in a PEM Fuel Cell [3]- *anode, cathode, electrolyte and catalyst*. The anode, the negative post of the fuel cell, has several functions. It conducts the electrons that are freed from the hydrogen molecules so that they can be used in an external circuit. It has channels etched into it that disperse the hydrogen gas equally over the surface of the catalyst. The cathode, the positive post of the fuel cell, has channels etched into it that distribute the oxygen to the surface of the catalyst. It also conducts the electrons back from the external circuit to the catalyst, where they can recombine with the hydrogen ions and oxygen to form water. The electrolyte is the proton exchange membrane. This specially treated material only conducts *positively charged ions*. The membrane blocks electrons. For a PEMFC, the membrane must be hydrated in order to function and remain stable. Finally, the catalyst is a special material that facilitates the reaction of oxygen and hydrogen. It is usually made of platinum nanoparticles very thinly coated onto carbon paper or cloth. The catalyst is rough and porous so that the maximum surface area of the platinum can be exposed to the hydrogen or oxygen. The platinum-coated side of the catalyst faces the PEM. As the name implies, the heart of the cell is the proton exchange membrane. It allows protons to pass through it virtually unimpeded, while electrons are blocked. When the H_2 hits the catalyst and splits into protons and electrons (a proton is the same as an H^+ ion) the protons go directly through to the cathode side, while the electrons are forced to travel through an external circuit. Along the way they perform useful work (e.g. lighting a bulb or driving a motor) before combining with the protons and O_2 on the other side to produce water. Pressurized hydrogen gas (H_2) entering the fuel cell on the anode side. This gas is forced through the catalyst by the pressure. When an H_2 molecule comes into contact with the platinum on the catalyst, it splits into two H^+ ions and two electrons (e^-). The electrons are conducted through the anode, where they make their way through the external circuit (doing useful work such as turning a motor) and return to the cathode side of

the fuel cell. Meanwhile, on the cathode side of the fuel cell, oxygen gas (O_2) is being forced through the catalyst, where it forms two oxygen atoms. Each of these atoms has a strong negative charge. This negative charge attracts the two H^+ ions through the membrane, where they combine with an oxygen atom and two of the electrons from the external circuit to form a water molecule (H_2O). All these reactions occur in a so-called *cell stack*. The design also involves the setup of a complete system around the core component that is the cell stack. The stack will be embedded in a module including fuel, water and air management, coolant control hardware and software. This module will then be integrated in a complete system to be used in different applications. Due to the high energetic content of hydrogen and high efficiency of fuel cells (55%), this great technology can be used in many applications like transport (cars, buses, forklifts, etc) and backup power to produce electricity during a failure of the electricity grid. As noted earlier, Toyota corporation has led the development of PEM hybrid fuel cells for automobiles. “Mirai” means *the future* in Japanese, and is the name is given to Toyota’s new vehicle design which is a regular mid-size, four-door sedan. Toyotas new vehicle uses fuel cell system technology, giving it an extremely advanced powertrain compared to standard vehicles in current time. This design is the world’s first vehicle design powered by a fuel cell stack unit with zero powertrain emissions. The type of fuel cell used in this model is a PEM (**Fig. 2**).

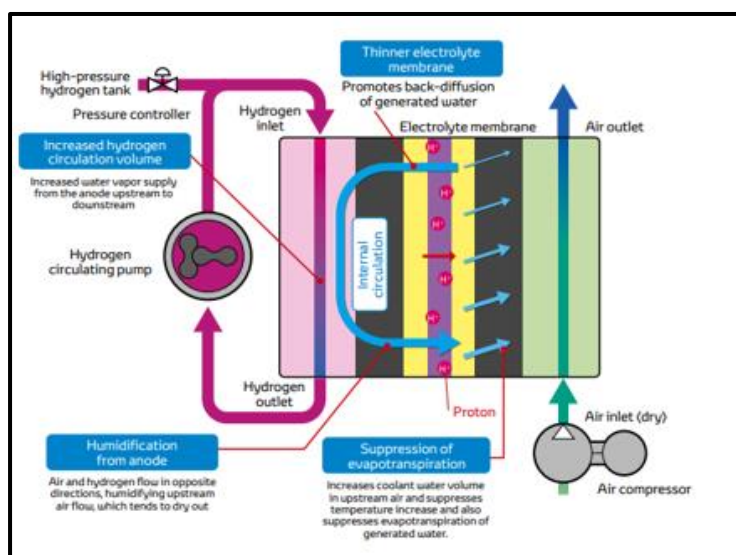


Fig 2: Toyota Mirai PEM fuel cell (courtesy Toyota-Japan)

The schematics of the fuel cell individual module is illustrated above. The engine bay is a 152 bhp electric motor and the Mirai model is a front-wheel drive via single speed gearing. Behind it are two high-pressure hydrogen tanks (One for storage and one for expansion) and a high voltage nickel metal hydride drive battery. The Mirai is capable of regenerating and storing energy under the braking like any other standard Toyota vehicle. On a full tank of hydrogen, the vehicle can compete with a similar engine/tank sized petrol car. Refueling the vehicle takes between 3-5 minutes, and the after the vehicles was tested it was proven that it is a strong performance, smooth drive and quiet car with no tailpipe emissions other than water vapor. The vehicle weight fits within the range of standard sedan vehicles such as Ford Mondeos and Toyota Avensis. Even with the advanced power train technology the total weight of the vehicle is 1.8 tonnes, which is approaching what a beam axle can be expected to suspend without any compromise to either ride or handling [4]. The hydrogen tank is the main issue when designing fuel cell units for vehicles, but Toyota developed its own wove carbon fiber tank which contains the hydrogen to fuel the fuel cell unit. The size of the fuel cell itself is similar to conventional petrol tank and it sits under the front seats, and the fuel cell has the ability to work at cold-starts as low as $-30^{\circ}C$. the positioning of the hydrogen tank and fuel cell module is shown in **Fig. 3**.

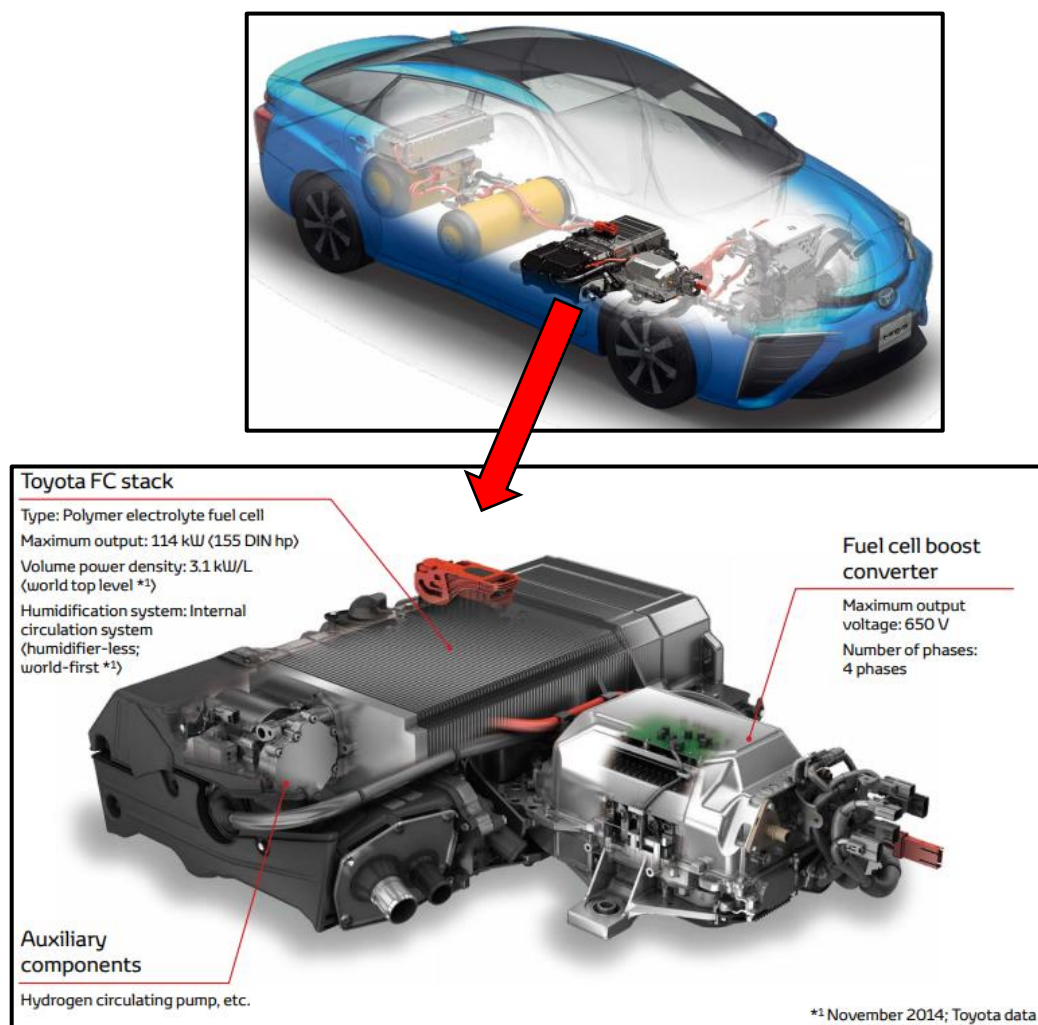


Fig 3: PEM fuel cell in the Toyota Mirai (courtesy Toyota-Japan)

Furthermore, the cells operating principles are outlined in a step by step procedure, demonstrated in **Fig. 4**. The main components required to make the Mirai a functioning fuel cell – electric vehicle, are displayed in **Fig. 5**. Overall, the main problem faced when designing a fuel cell is the sizing and pressurizing the hydrogen tank. Various companies have solved this problem and patented designs. However, as shown in the fuel cell designs that currently exist are used in relatively larger application bodies compared to vehicles. There are not many automotive vehicles manufacturers that have successfully patented fuel cell powered cars. Companies such as Ford are currently in the process of completing a fuel cell drive system. The current existing design by Ford is for the transit van, as it is a large body and all components can fit. Japanese engineering is known worldwide and Toyota being the global lead vehicle manufacturing company have developed a compact sedan sized vehicle which is powered by a fuel cell. This has set the blueprint for all other corporations in the 21st century.

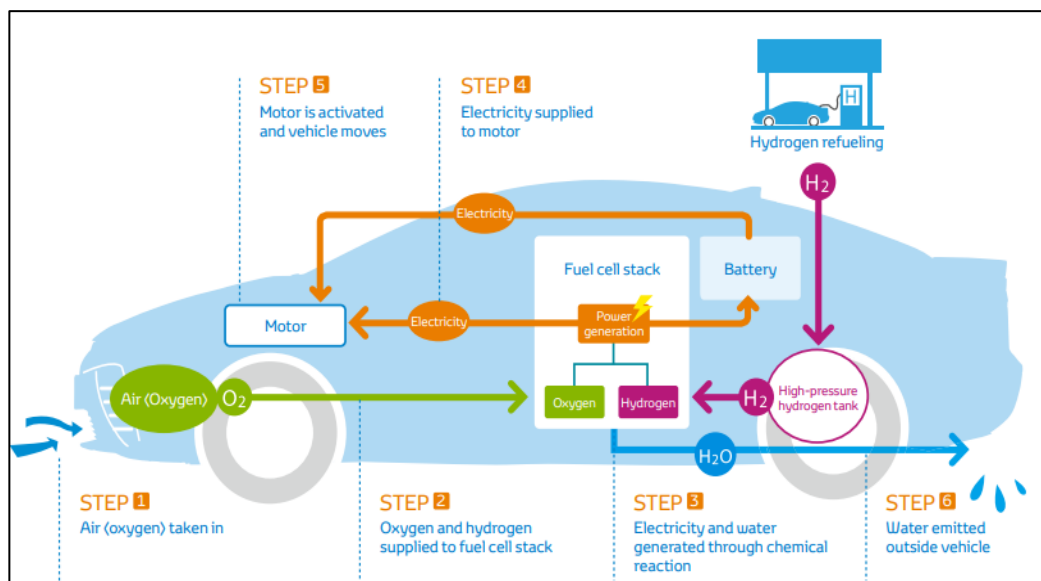


Figure 4: Fuel cell operation stages

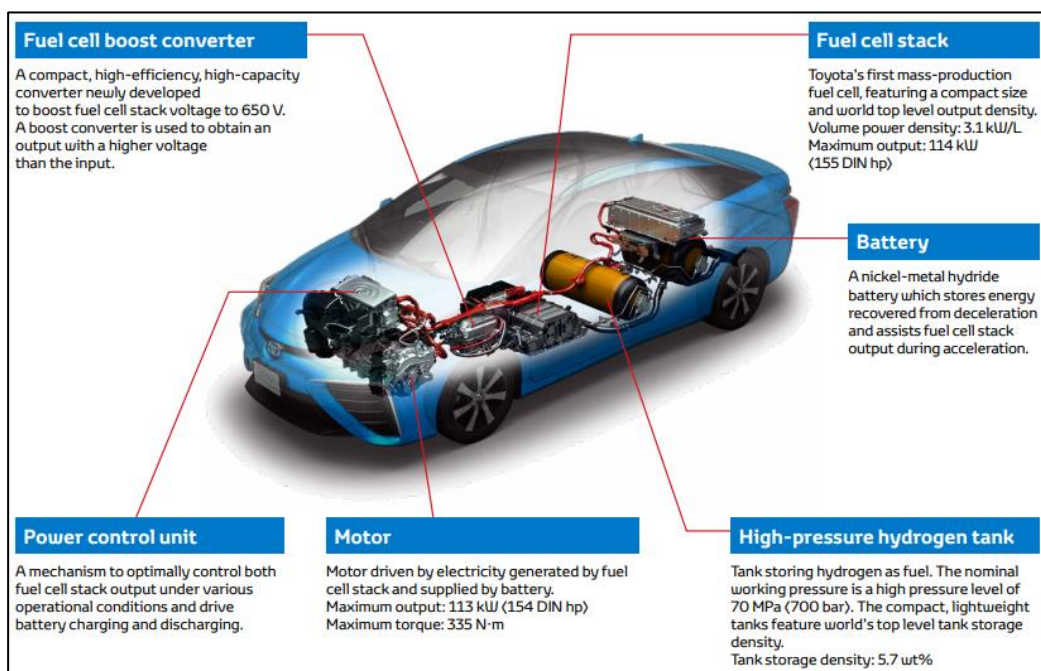


Figure 5: PEM Fuel cell integrated engineering in the Toyota Mirai

An important contribution to the fuel cell revolution has been the implementation of computational fluid dynamics simulation. CFD [5] provides an inexpensive and powerful method for predicting many aspects of fuel performance. In conjunction with experimental testing, it is the leading tool used in engineering fluid dynamics in the 21st century. In the automotive sector, many different codes are used. Fuel cell technology has various modelling methods since it features both structural and fluid flow phenomena. There are various simulation tools that are capable of landscaping fuel cell geometries and achieving theoretical predictions of fuel cell performance. Simulation packages are useful and cost/time effective tools that require an input, in return giving an output that satisfies the objective. Some examples of automotive-applied CFD packages include AVL Fire which is capable of simulating fluid dynamic problems that involve complex geometries and advanced physics and/or chemistry. The electrified technology is a

programming language that is a multi-purpose thermo-fluid CFD software package, which defines both the powertrain and the automotive industry. Multiphase flow modules contain the Lagrangian and Eulerian multiphase modules. The Lagrangian multiphase modules entails the droplet break-up turbulence dispersion, coalescence, collision, drag, evaporation and distortion as well as the droplet-wall interaction. The Eulerian multiphase modules consider modelling the multi-fluid of the multiphase flow, thus solving the calculation of the volume fraction distribution for all flow variables in addition to each phase. Another code is CFD-ACE+ that provides coupled simulations of thermal, fluid, chemical phenomena. The software is designed for high performance workstations and clusters for parallel computing. However, the package is also utilized on normal computers. The software package entails built-in electrochemical models which can be further developed, i.e. manipulating the flow through porous media and small channels. Fuel cell modules account for the fundamental physics of fuel cells, and the package includes a model for water transport via the membrane. The package includes a sample model for transport of liquid water saturation through a porous media and the liquid saturation example model for two/multi-phase flow in the channels. COMSOL Multiphysics is adaptable programming platform for various coupled phenomena and uses finite element methods. The underlying electrochemical phenomena can be modelled using the electrolytes and electrodes provided by fuel cell and battery modules. The CFD module gives an understanding of flow in porous media as well as multiphase flows. The model is created using the multiphase mixture, Eulerian-Eulerian multiphase models or the bubbly flow. To highlight and describe the phase changes, the built-in step functions are utilized. The most popular software for commercial CFD remains ANSYS Fluent which is a versatile but general-purpose fluid analysis simulation package, with a wide range of physical modelling capabilities for modelling turbulence heat transfer, flow and reactions for industrial applications. The electrochemistry, mass and current transportation, liquid water formation and heat source can be modelled using this software as the fuel cell module is provided as a built-in feature. To calculate the multiphase flow, two distinct approaches are utilized- Eulerian-Eulerian and Eulerian-Lagrangian. When using the Eulerian-Eulerian method the various phases are treated mathematically as inter-penetrating continua. In the fluent version of the ANSYS software there are three Eulerian-Eulerian multiphase models available; the mixture model, VOF model and the Eulerian model. On the contrary, in the Eulerian-Lagrangian approach the multiphase fluid is treated as a continuum by solving Navier-Stokes equations, although the dispersed phase is solved by tracing a large number of bubbles, particles or droplets, which is attained by calculating the flow field. Finally, OpenFOAM is a diverse open source CFD code, that can solve various problems from solid dynamics and electromagnetics to complex fluid flow which include chemical reactions, heat transfer and turbulence. The object-orientated design of the programming language was written in C++, which authorizes the user to develop and implement their own numerical algorithms and models. The program is known for its adaptability as the user has complete freedom to customize and extend all existing functionalities. The approach to solve multiphase flows ranges from a system with one phase dispersed to two fluid phase model via VOF phase fraction-based interface capturing approach, to multi-fluid models and multiphase mixture. Macedo-Valencia *et al.* [6] employed ANSYS FLUENT to simulate single-phase, three-dimensional fluid flow, heat transfer, electrochemical reaction and species transport in a Proton Exchange Membrane Fuel Cell stack with five single cells including the membrane, gas diffusion layers, catalyst layers, flow channels and current collectors. They observed that the species concentration is invariably higher at inlets and is reduced gradually along the channels. Furthermore, they found that minimal temperature arises at the inlet of the cathode where oxygen is supplied at temperature of 300 K. Likewise, the heat sources in PEM fuel cell are strongly interdependent on the current density distributions through membrane electrodes assembly. Awotwe *et al.* [7] employed ANSYS CFX to study effect of varying the flow rate (i.e. velocity) on the pressure drop in bi-polar plate design of PEM fuel cells. They noted that a reduction in pressure drop contributes to the improvement of performance; however, many other electrochemical and geometric factors also

influence overall performance of the cell and reduction in pressure drop alone is not sufficient. In addition to these codes, many other approaches have been adopted for PEM fuel cell CFD simulation. For example, Ravishankar *et al.* [8] presented three-dimensional numerical computations of cooling channel designs based on traditional serpentine and spiral designs for a PEM fuel cell, using a streamline upwind/Petrov Galerkin finite element method for Reynolds number ranging from 415 to 1247. They observed that hybrid designs achieve improved performance compared to serpentine geometries in terms of uniformity in temperature distribution at all Reynolds numbers. Many other approaches have been explored including molecular dynamics (MD) simulation, although it is computationally very expensive [9]. Other interesting studies of CFD modelling of PEM fuel cells are reported in [10]-[20]. In the current presentation, the ANSYS FLUENT workbench software is deployed to simulate flow characteristics and temperature distributions in a 2-dimensional enclosure replicating a hybrid PEM hydrogen-oxygen fuel cell. Extensive visualization of transport phenomena in the fuel cell is included i.e. streamline and isotherm contours in addition to density distribution. Validation of the finite volume computations has also been achieved with a thermal Lattice Boltzmann method (LBM) [21] achieving excellent agreement. Mesh independence tests are also performed. The simulations constitute a first step in understanding more deeply the intrinsic transport convection characteristics of PEM hydrogen-oxygen fuel cells.

2. ANSYS FLUENT CFD MODEL

To simulate a full PEM fuel cell is very challenging and requires usually of the order of millions of elements (finite volumes). It is common in commercial groups to simulate in 3-dimensions the PEM fuel cell and compute velocity and pressure drops with multi-million density meshes. In this presentation, however, owing to mesh limitations, attention is restricted to a two-dimensional model of a moving membrane PEM fuel cell. Simulations are executed in ANSYS FLUENT version 19.

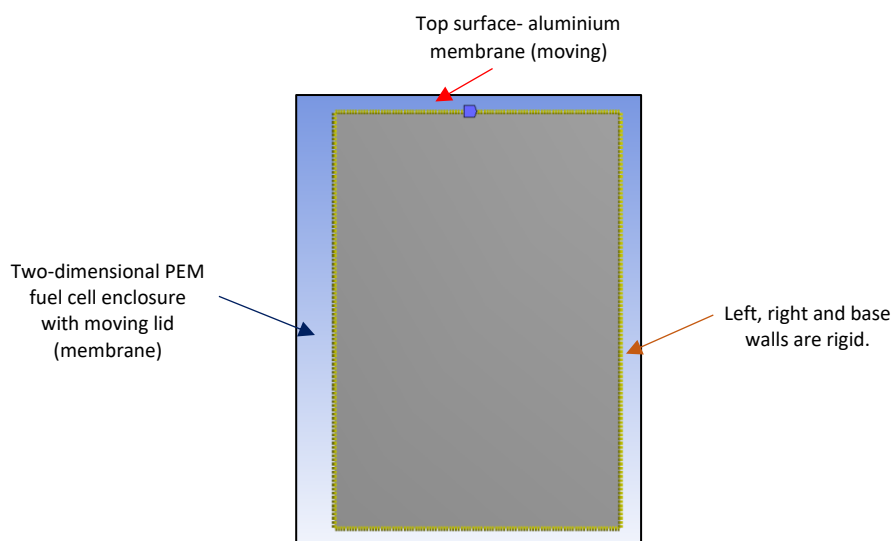


Fig 6: Model for PEM fuel cell with membrane upper wall

The focus is on laminar, viscous convection flow to compute heat flux variation, change in streamline (isovelocity), pressure and temperature for five various fuel cells in a layer of the fuel cell which has a moving membrane and both hydrogen and oxygen are introduced to the cell. Electrochemistry is ignored in these simulations and is the subject of a subsequent study [22]. The mathematical model employed in ANSYS FLUENT is next elaborated, followed by simulations.

Mass Conservation Equation

The unsteady equation for mass conservation or continuity is written as follows:

$$\frac{\partial \rho}{\partial t} + \nabla \cdot (\rho \vec{v}) = S_m \quad (1)$$

The equation above is the general form of the mass conservation equation which is valid for both compressible and incompressible flows. The source S_m is the mass (kg) applied to the continuous phase from the dispersed second phase and any user-defined sources. Here (\vec{v}) is the velocity vector in three dimensions, ρ is fluid density (kg/m³), t is time (s).

Momentum Conservation Equation

Conservation of momentum in an inertial (non-accelerating) reference frame takes the form.

$$\frac{\partial}{\partial t} (\rho \vec{v}) + \nabla \cdot (\rho \vec{v} \vec{v}) = -\nabla p + \nabla \cdot (\bar{\tau}) + \rho \vec{g} + \vec{F} \quad (3)$$

Where, p is the static pressure (Pa), $\bar{\tau}$ is the stress tensor (N/m²), $\rho \vec{g}$ and \vec{F} are the gravitational body force (N) and external body force (N) e.g. thermal buoyancy, respectively (e.g. arising from interaction with the dispersed phase). \vec{F} also has other model-dependent source terms such as user-defined sources and porous-media. The $\bar{\tau}$ term is given by:

$$\bar{\tau} = \mu \left[(\nabla \vec{v} + \nabla \vec{v}^T) - \frac{2}{3} \nabla \cdot \vec{v} I \right] \quad (4)$$

Here μ is the dynamic viscosity (kg/(ms)), I is the unit tensor and the last term shown is the effect of volume dilation. No slip velocity conditions are applied at the rigid walls and a moving boundary velocity at the top wall.

To simulate thermal convection heat transfer in the PEM fuel cell, ANSYS permits applying the heat transfer function within the fluid/solid body of the model, where problems can range from thermal mixing within a fluid to conduction in composites. To apply heat transfer to the actual model, thermal boundary conditions should be supplied to the body and material properties should be inserted that govern heat transfer. ANSYS Fluent solves the energy transport (heat) using the general equation:

$$\frac{\partial}{\partial t} (\rho E) + \nabla \cdot (\vec{v} (\rho E + p)) = \nabla \cdot [k_{eff} \nabla T - \sum_j h_j \vec{J}_j + (\bar{\tau}_{eff} \cdot \vec{v})] + S_h \quad (5)$$

Here k_{eff} is the effective conductivity ($k + k_t$, where k_t is the thermal conductivity). \vec{J}_j is the diffusion of flux species j . S_h is the heat produced due to the chemical reaction and any form of volumetric heat source. The remainder terms on the right side of the equation show the energy transfer due to species conduction, species diffusion and viscous dissipation respectively. Ofcourse when electrochemistry is neglected the flux species term is neglected. The energy transport equation in solid regions (thermal conduction), within ANSYS Fluent has the following form:

$$\frac{\partial}{\partial t}(\rho h) + \nabla \cdot (\vec{v}\rho h) = \nabla \cdot (k\nabla T) + S_h \quad (6)$$

Here k is material (wall) conductivity, T is the temperature of body (K), S_h is the volumetric heat source, ρ is the density of material (kg/m^3) and h is enthalpy (J/kg). In this study we consider the thermal convection flow in a 2-D PEM fuel cell. This allows the simulation of general internal circulation in the fuel cell. Although the 2D mesh does not consider the third dimension it enables a comprehensive understanding of the behavior of the two gases in the fuel cell membrane (oxygen and hydrogen). Heat is added to the bottom wall of the fuel cell as the top wall is a moving membrane to illustrate the oxygen and hydrogen flow valves. The bottom wall is heated to mirror the heat energy dissipated to surroundings once the hydrogen and oxygen molecules enter the center chamber (membrane). The opposite reaction to the heat dissipation is the actual heat which is supplied to the fuel cell wall itself. This analysis monitors the behavior of hydrogen and oxygen within the membrane when heat is applied. The parameters analyzed are:

- i. Heat Flux
- ii. Temperature
- iii. Pressure
- iv. Streamline velocity

The parameters prescribed in the model are extensive and summarized in **Table 1**. Boundary conditions prescribed are listed in **Table 2**.

Material	Hydrogen	Oxygen
Density ρ (kg/m^3)	1.2999	0.08189
Specific Heat C_p (J/kg-K)	Piecewise-Polynomial	Piecewise-Polynomial
Thermal Conductivity (w/m-K)	0.0246	0.1672
Dynamic viscosity μ (kg/ms^{-1})	1.919×10^{-5}	8.411×10^{-6}
Molecular Weight (kg/mol)	31.9988	2.01594
Standard State Enthalpy (J/kgmol)	0	0
Standard State Enthalpy (J/kgmol-K)	205026.9	130579.1
Reference Temperature (K)	298.15	298.15
Thermal Accommodation Coefficient	0.9137	0.9137
Momentum Accommodation Coefficient	0.9137	0.9137
Critical Temperature (K)	154.58	32.98
Critical Pressure (Pa)	5043000	1293000
Critical Specific Volume (m^3/kg)	0.002293	0.031846
Acentric Factor	0.021	-0.217

Table 1: Data specification in ANSYS FLUENT

Boundary Condition	(Temperature °K)	Velocity
Moving Membrane (Top Wall)	-	1 m/s
Left Wall	300	- (no slip)
Right Wall	300	- (no slip)
Bottom Wall	353, 473 and 1273	- (no slip)

Table 2 – Velocity and Thermal Boundary Conditions

Membrane Wall Properties	
Length (m)	0.3
Width (m)	0.2
Material	Aluminum
Density of Aluminum (kg/m ³)	2700
Mass of Membrane (kg)	0.162

Table 3: Moving membrane (top wall) material properties

To apply the ANSYS theory and determine the behavior of the two gases within the fuel cell, ANSYS Fluent was utilized. The CFD solver can be run in or outside the workbench environment. To begin the design procedure, the parameters and dimensions of the fuel cell model were researched. Although, the patented models in existence do not provide dimensions of the fuel cell as the information is classified, dimensions were attained by analyzing the stack fixture within an actual vehicle. The dimensions were then researched upon, which showed similarity between the predicted dimensions measured from the stack geometry thus, giving the fuel cell membrane the dimensional image, it has. The modelling procedure was conducted in four stages- geometry, mesh, setup (pre-processing), solution (processing) and results (post-processing). A 2-D x-y geometric model is designed (**Fig. 7**). Once the membrane shape was outlined the dimensions were specified as shown. The next step was to create a surface body in the main toolbox and select surfaces from sketches.

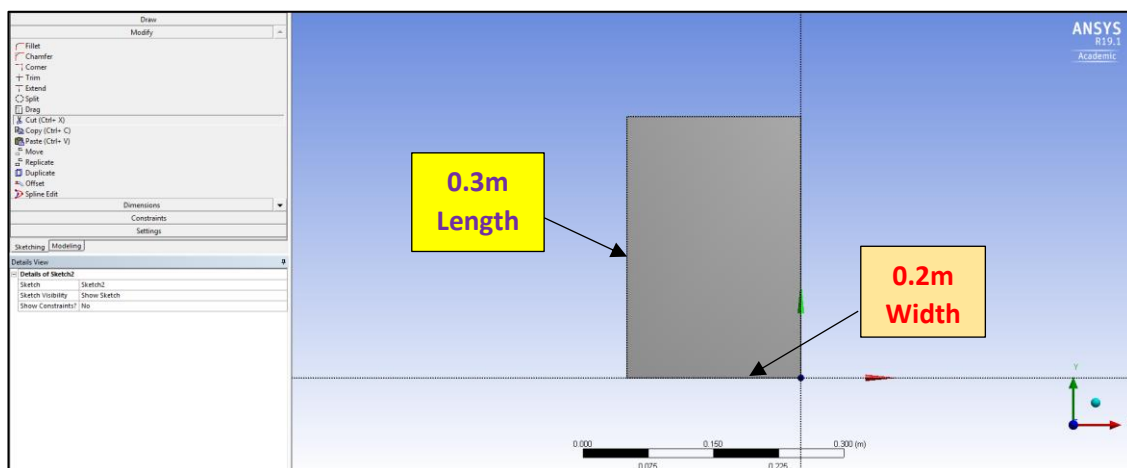


Figure 7: ANSYS PEM Fuel cell Geometric model

Number of Contours	Number of Divisions	Number of Elements
100	100	10100

Table 4: Mesh selection study

The mesh is initially designed using a coarse density with quadrilateral elements. It is then refined to achieve mesh (grid) independence. 10,100 elements are finally utilized in the mesh, as shown in **Table 4** and **Fig. 8**.

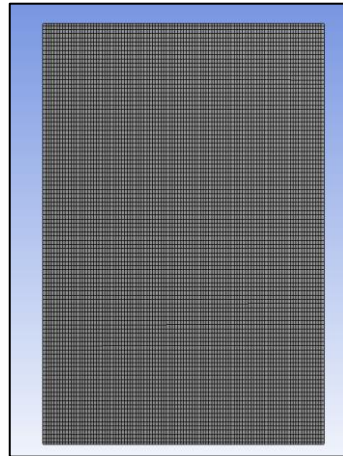


Fig 8: PEM fuel cell mesh

In the analysis “setup”, the following are specified: Processing Options – Serial, Display Options – Enable both display mesh after reading and workbench color scheme and Options – Ensure double precision is disabled and dimensions is pre-selected on 2D. The pressure-based solver is selected (since incompressible flow is considered in the PEM fuel cell), (planar) steady state time response is adopted, and the number of iterations is selected as 2000 to ensure convergence and accuracy. In the general setup, viscous laminar, single-phase flow with energy is selected (“radiation” and “multiphase” options are de-selected). Within the general setup window, the fuel cell model is meshed in a steady-state time response in planar spatial dimensions. The velocity formulation option selected is the “absolute velocity” as the gases within the membrane are monitored, whereas, the relative velocity option shows the moving membrane (top wall) which effects the behavior of the gas and describes inaccurate results. If electric fields were applied the relative velocity would be the parameter to be analysed, however this is not considered here. The hydrogen and oxygen entering is not “compressed” so the pressure-based model (solver) is appropriate. The next step is to add “material” on the membrane body. The first simulation for the fuel cell membrane is with hydrogen and the subsequent analysis is conducted with oxygen. ANSYS Fluent has its own database which enables the user to choose the material. The material properties such as density ρ (kg/m^3), specific heat C_p (J/kgK), thermal conductivity (W/mK) and dynamic viscosity μ (kg/ms^{-1}), are automatically adjusted once the material is chosen from the data base. The next stage involves applying boundary conditions (**Table 2**). An initial boundary condition was applied to the moving membrane (top wall). Similarly, the same steps were followed ensuring all other surfaces (left, right, base walls) of the body have a no-slip boundary condition. Furthermore, the right and left wall as well as the moving membrane have a thermal boundary condition of room temperature at approximately 300°K . However, the base walls temperature is varied in the simulations between 80°C (353°K) to 200°C (473°K) and finally 1000°C (1273°K). The bottom wall was treated as a heat source due to the thermal energy dissipating from the fuel cell body when the current is extracted. The temperatures represent the thermal boundary condition at which the PEM, SOFC and AFC/PAFC fuel cells modules work when powering any device/s. The solver stages are summarized in **Figs. 9a, b** for the “methods” and “controls” selected.

Solution Methods	Solution Controls
Pressure-Velocity Coupling	Under-Relaxation Factors
Scheme SIMPLE	Pressure 0.3
Spatial Discretization	Density 1
Gradient Least Squares Cell Based	Body Forces 1
Pressure Standard	Momentum 0.7
Momentum Second Order Upwind	Energy 1
Energy Second Order Upwind	

Fig 9a, b: ANSYS FLUENT solver selection

As the calculation progresses the surface monitor history was plotted as shown in the graphics window above. The solution was automatically stopped by ANSYS Fluent once the residuals reached their specified value or after 2000 iterations. The number of iterations varies according to the platform utilized.

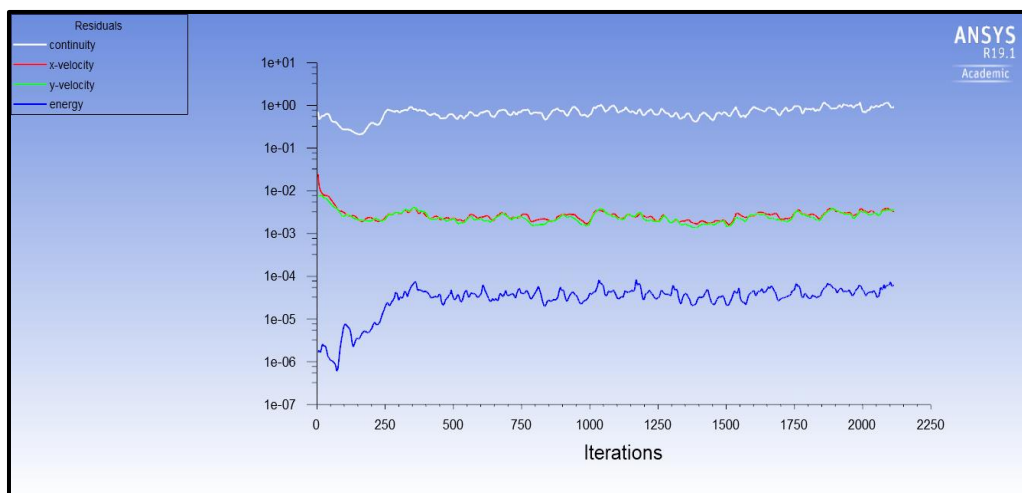


Fig 10: Residual iterations

3. CONVERGENCE STUDY

Extensive simulations have been conducted in ANSYS workbench. However, to ensure that the computations are accurate, a convergence and mesh independence study is carried out to determine the element size suitable for this model. We therefore describe the outlines when the results converge, and the division size chosen and highlight the model parameters and specifications. Mesh convergence is related to the size of the element (how small the element must be) to ensure the results produced from the CFD analysis, are not affected by changing mesh size. It is one of the key issues studied in computational fluid (and solid) mechanics, to analyse the affects it has on the accuracy of the results. A convergence study can be completed for both 2D and 3D problems, and the mesh is doubled each step, so an accurate comparison can be made. Convergence studies can be carried out on velocity, temperature, heat flux,

pressure etc. A minimum of three points need to be considered, and as the mesh density increases, the variable under consideration starts to converge to a specific value. If two subsequent mesh refinements do not alter the results substantially, then it can be assumed the results have converged and grid independence is said to be achieved.

Number of Divisions	Number of Elements	Heat Flux at 0.1m
40	1599	8591.78418
60	3600	8211.40723
80	6480	1919.6947
100	10100	1909.78406
120	14280	1899.80591

Table 5: Mesh independence study

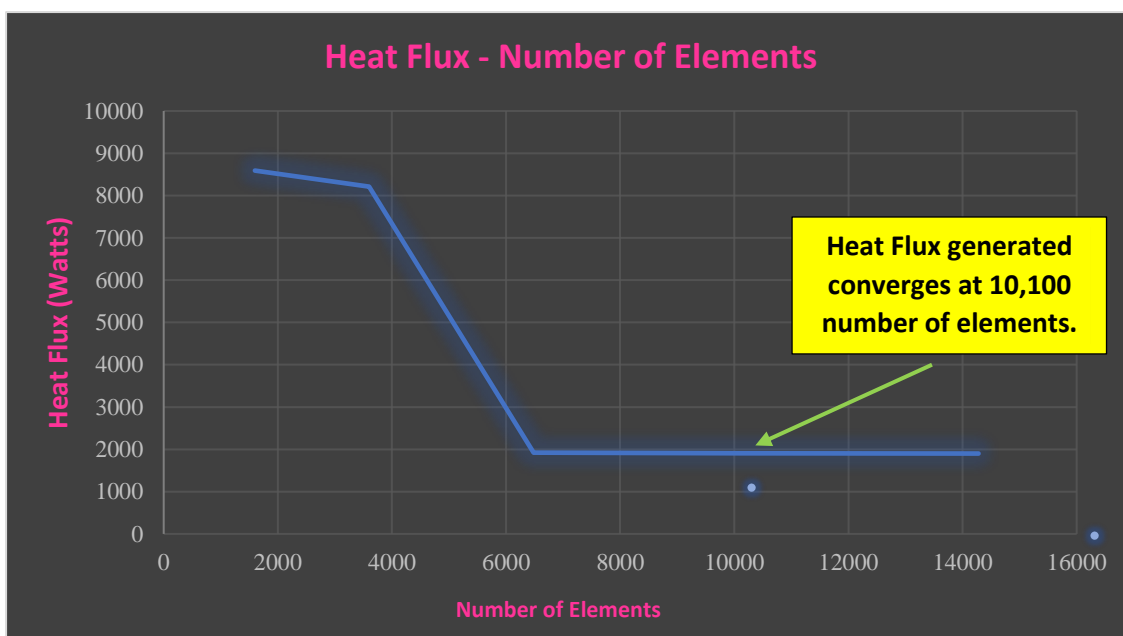


Fig. 11: Mesh independence graph

In all the subsequent computations, by selecting the contour and streamline options the image of the hydrogen/oxygen behaviour is portrayed, and the red-blue color highlights show the intensity of the parameter being analysed. In this case the three parameters analysed were temperature, pressure and streamline velocity. The parameter was changed from the variable section and after choosing a parameter i.e. density, the “apply cell” option is selected. This produces very clear and coherent visualization as shown in **Fig. 12**.

4. NUMERICAL RESULTS, VISUALIZATION AND DISCUSSION

Two gases are simulated within the fuel cell membrane- oxygen and hydrogen. Temperature, pressure and streamline (iso-velocity) contours are computed in addition to density distribution. The results are displayed below for both gases (Hydrogen and Oxygen) at various temperature

(353°K, 473°K and 1273°K). The temperatures illustrate the working temperature of the following fuel cell types:

- i. PEM Fuel Cell – Operation Temperature – 353°K (80°C)
- ii. AFC and PAFC Fuel Cell – Operating Temperature 473°K (200°C)
- iii. SOFC – Operating Fuel Cell – 1273°K (1000°C)

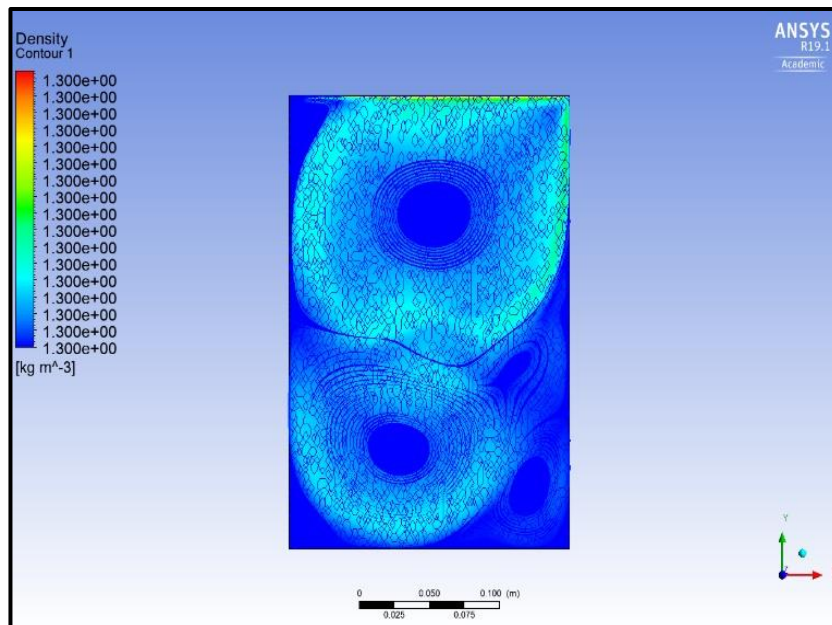


Fig. 12: Density distribution computation for simulations

Based on the mesh designed earlier, the ensuing plots depict *temperature, pressure, streamline* sets for the 3 different fuel cell configurations studied i.e. PEM fuel cell, AFC and PAFC Fuel Cell and SOFC (solid oxide fuel cell). In all the distributions, the common pattern highlighted by the results shows *asymmetrical dual vortices* with intense streamlines around the center points for both gases. The buoyancy effect (natural convection) occurs in the results shown by pressure plots for both oxygen and hydrogen gas for all three types of fuel cells. The buoyancy effect is an upwards force exerted by the fluid which opposes the weight of the immersed gas. In a column of fluid pressure increases with the depth owing to the weight of the overlying fluid (air). Thus, the pressure at the bottom of the column is greater than the top of the column. A high Nusselt number (ratio of convective to conductive heat transfer across the boundary) arises for the PEM and AFC/PAFC fuel cells in the temperature plots. In this study convection includes both advection and thermal diffusion. Additionally, with different gases, thermal properties change e.g. thermal conductivity, specific heat capacity and heat flux moves differently through the different gases. This explains the deviation in flow behaviour of both gases shown in the contour plots. As noted earlier, the top, right and left walls are at room temperature 300°K and the top wall i.e. moving membrane has a velocity of 1 ms⁻¹ representing the entry section.

Case 1: PEM fuel cell

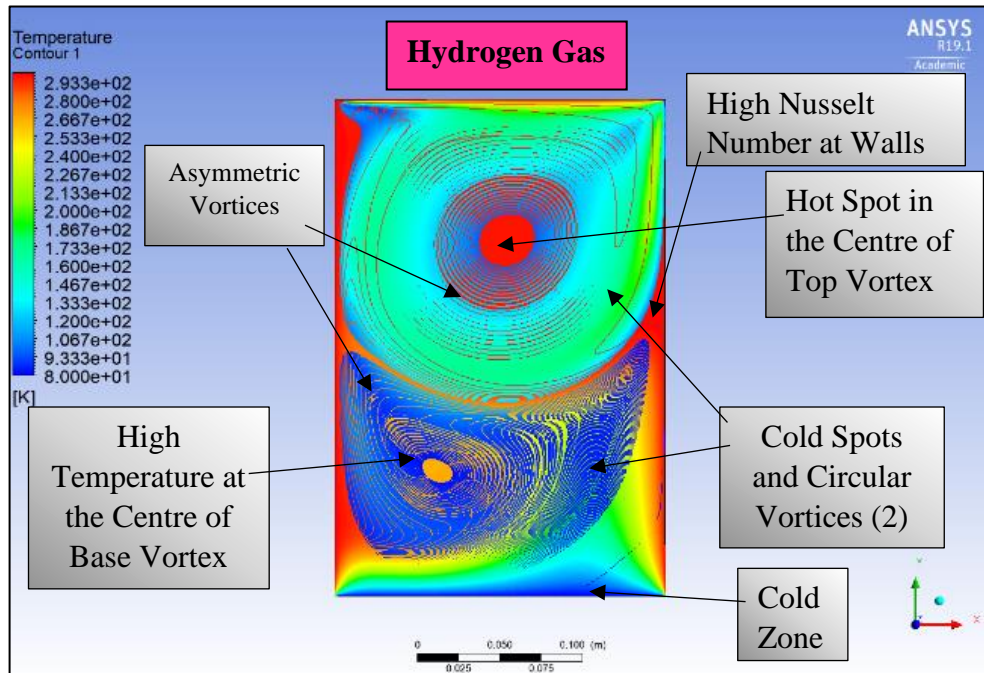


Figure 13a – Temperature Plot (Hydrogen)

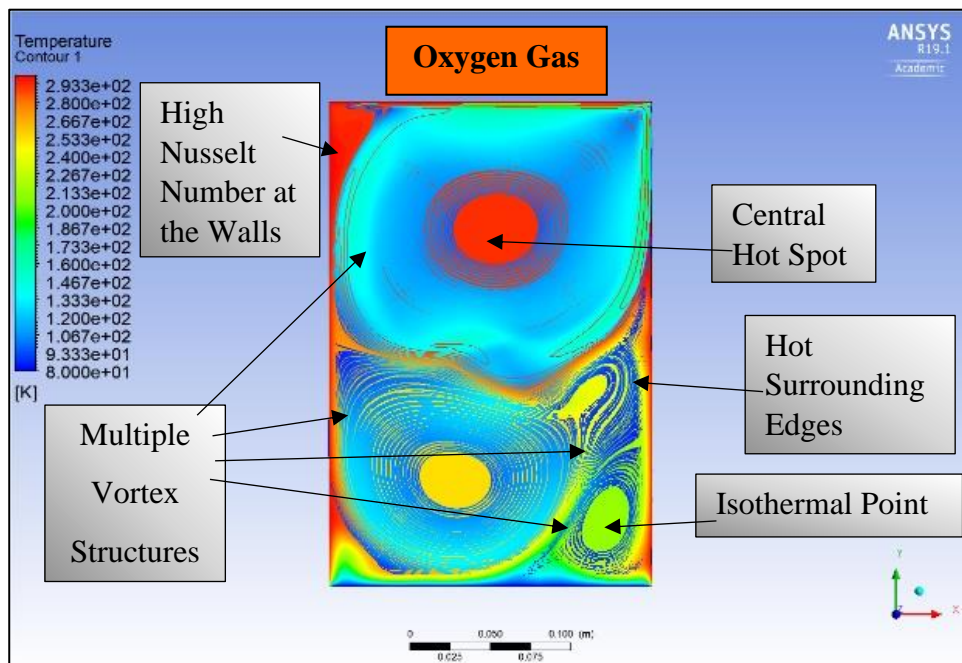


Figure 13b – Temperature Plot (Oxygen)

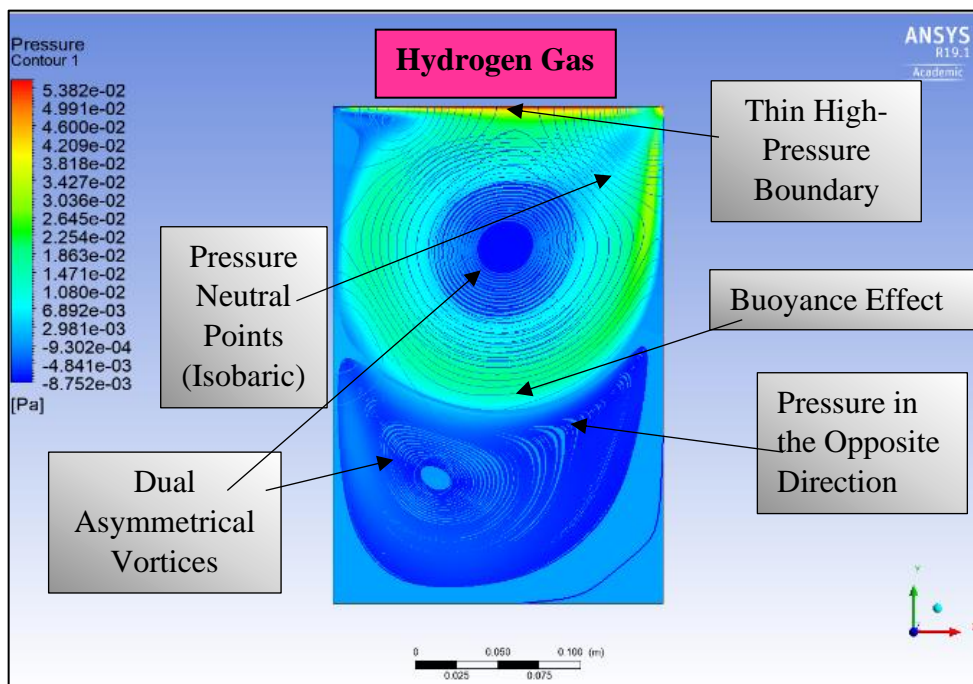


Figure 14a – Pressure contour distribution (Hydrogen)

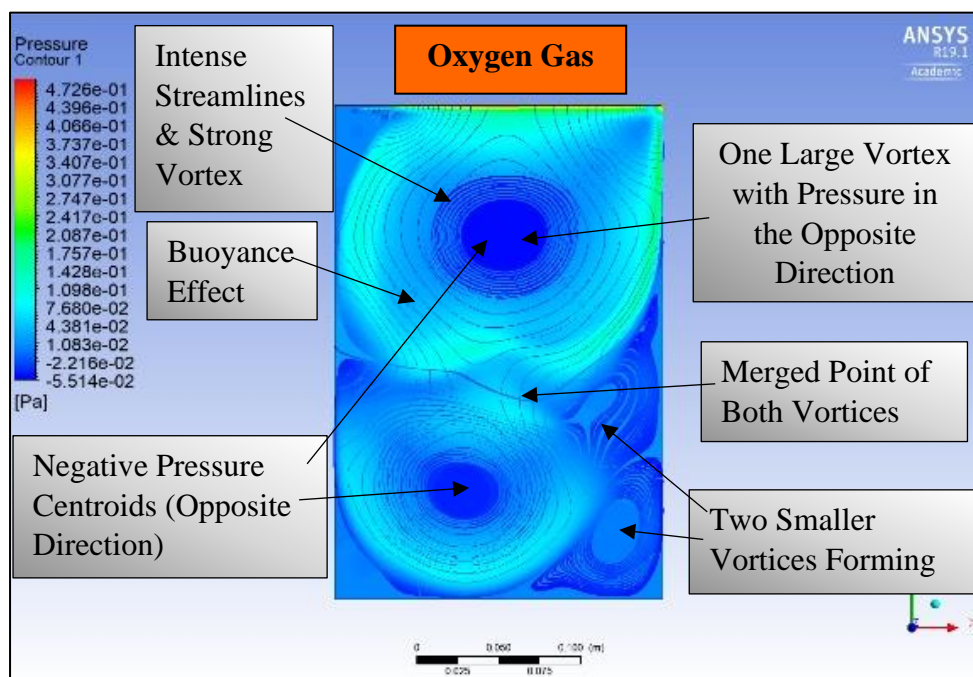


Figure 14b – Pressure contour distribution (Oxygen)

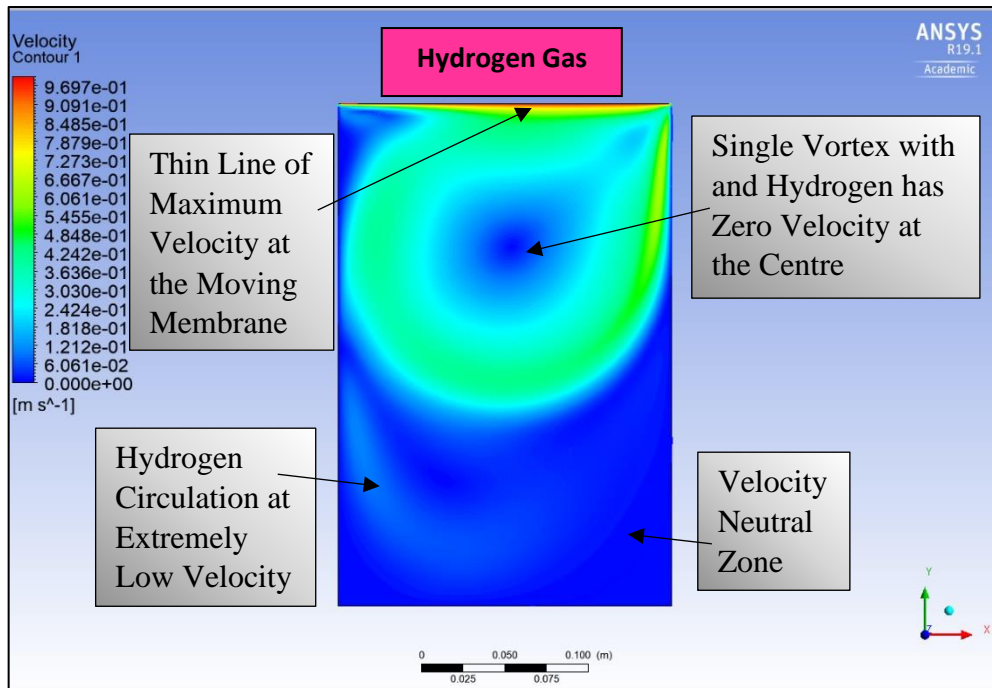


Figure 15a – Streamline contour distribution (Hydrogen)

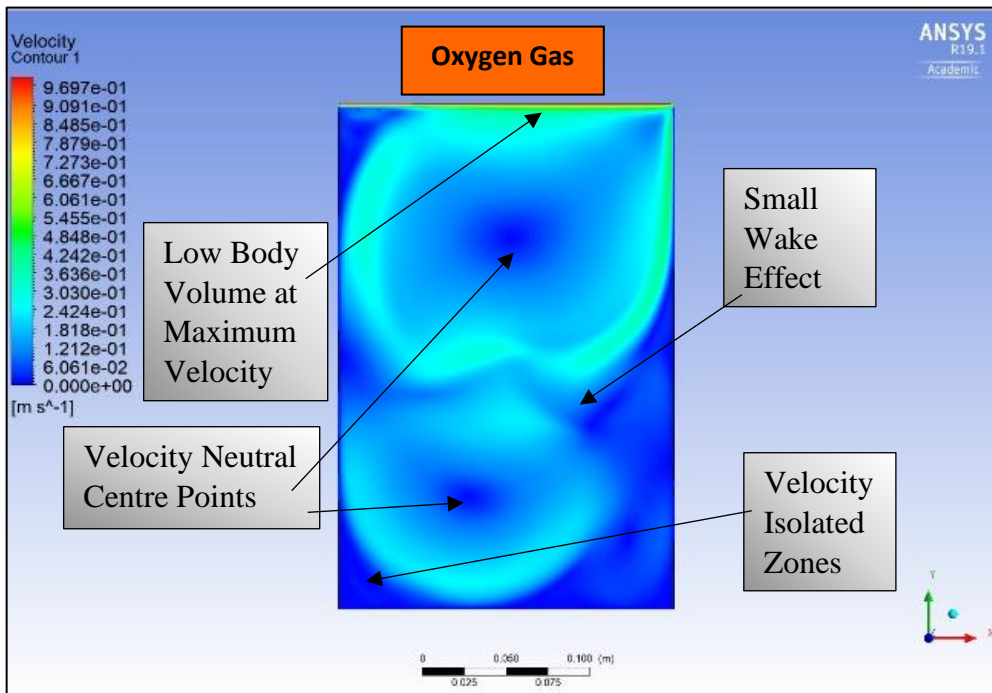


Figure 15b – Streamline contour distribution (Oxygen)

Case II: AFC/PAFC Fuel Cell

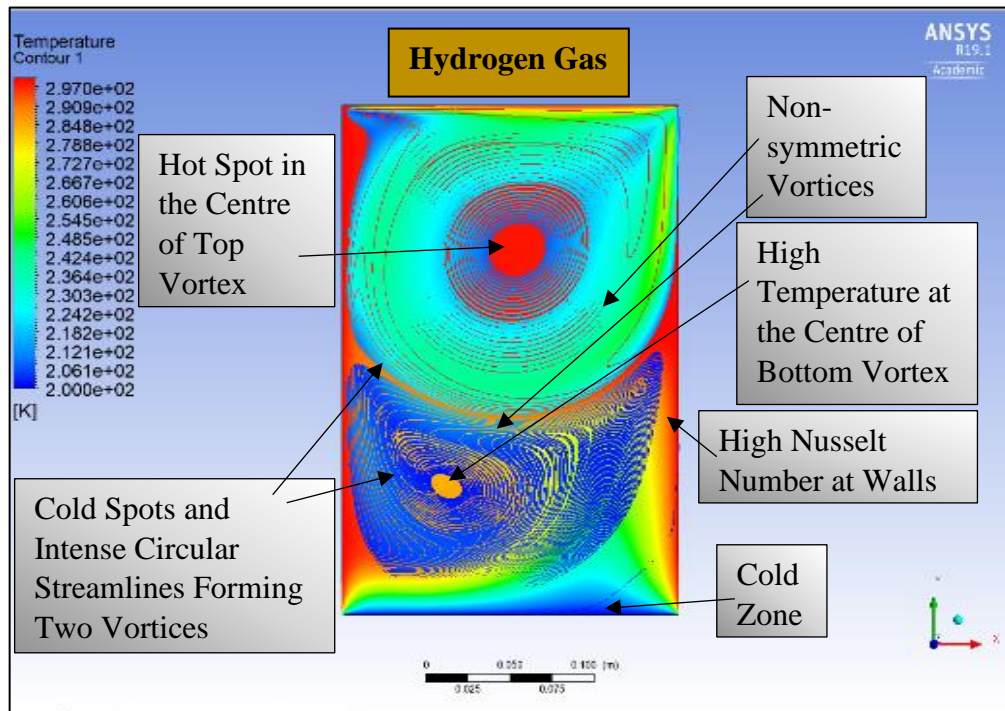


Figure 16a – Temperature contour distribution (Hydrogen)

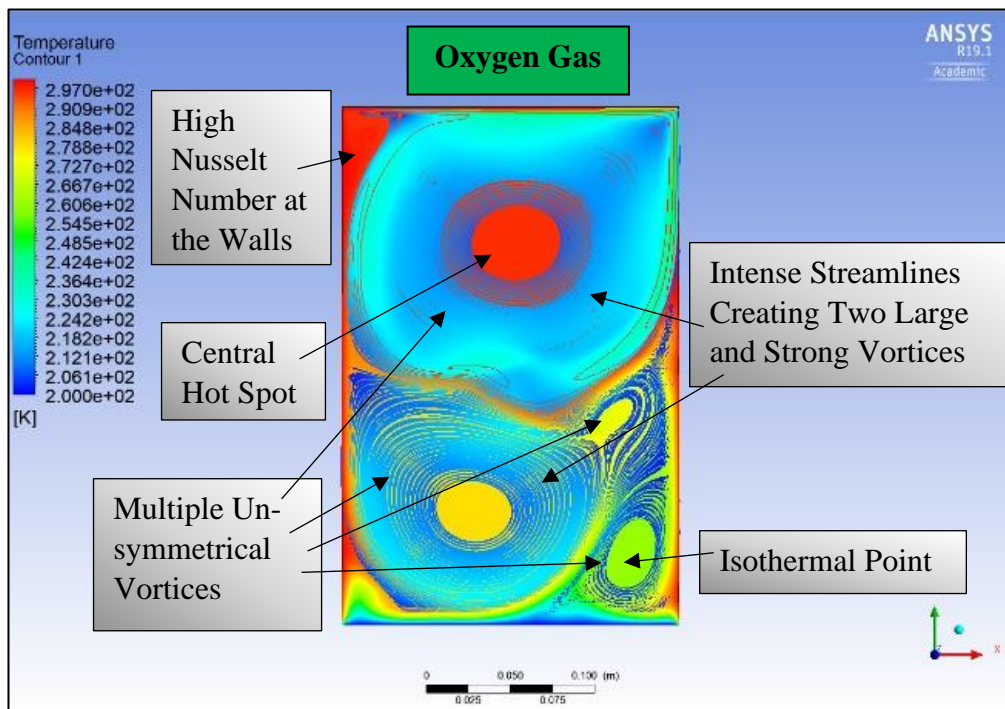


Figure 16b – Temperature contour distribution (Oxygen)

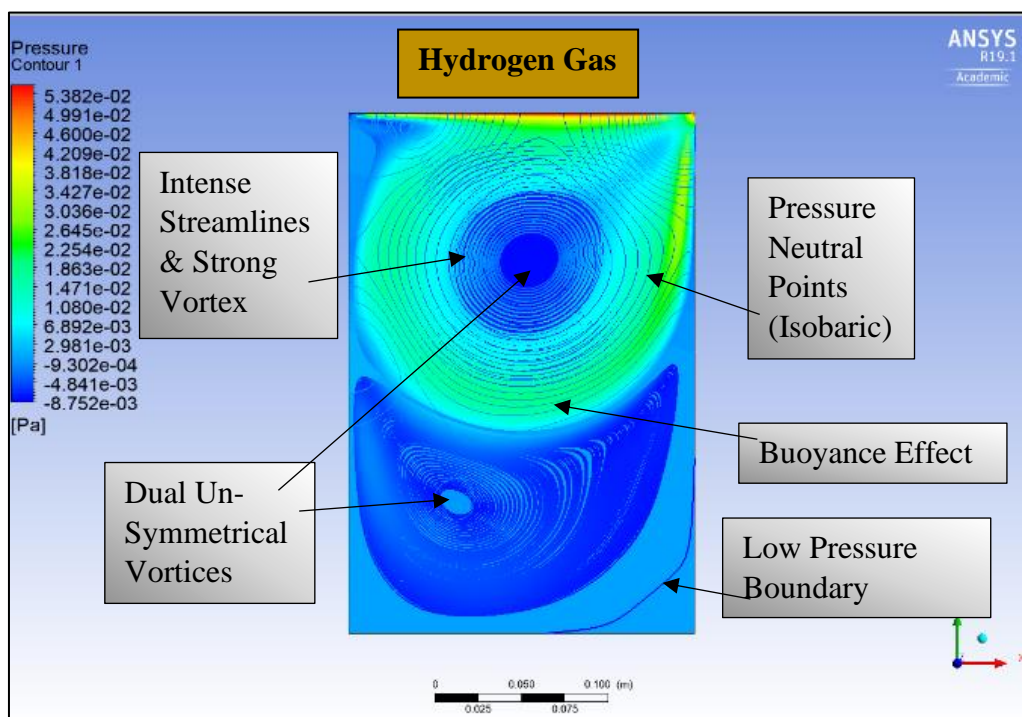


Figure 17a – Pressure contour distribution (Hydrogen)

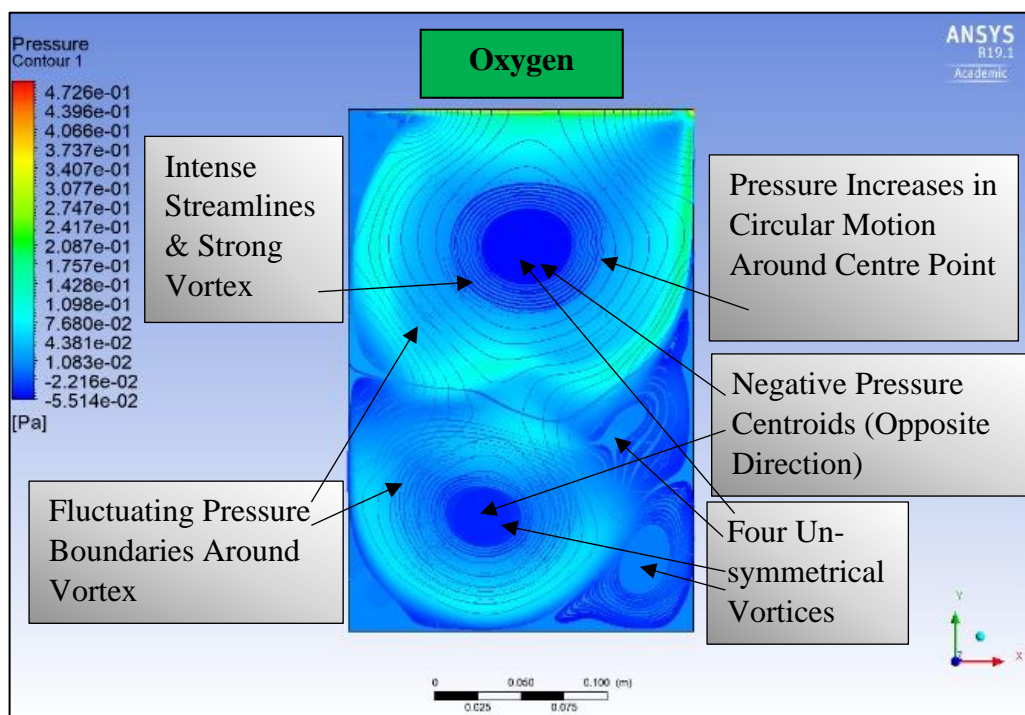


Figure 17b – Pressure contour distribution (Oxygen)

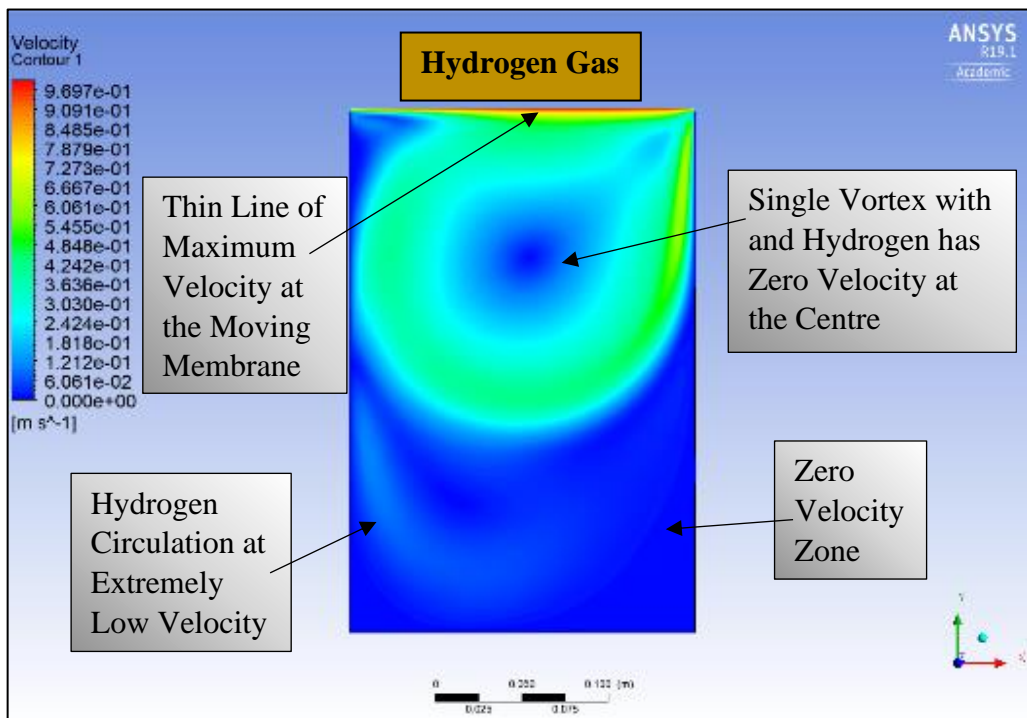


Figure 18a – Streamline (iso-velocity) contour distribution (Hydrogen)

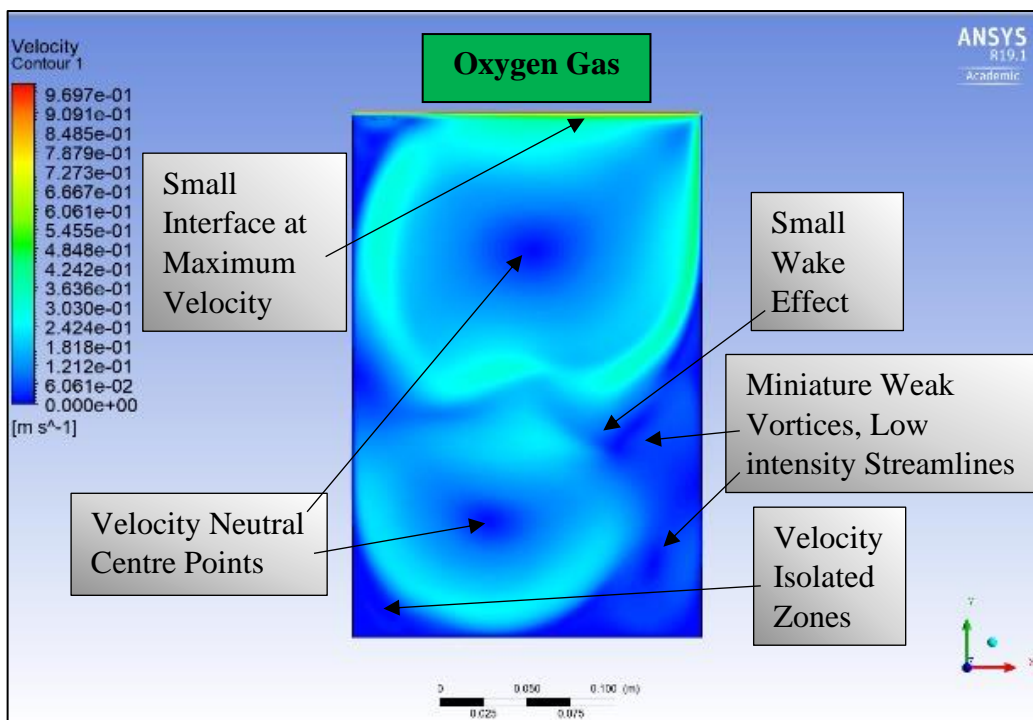


Figure 18b – Streamline (iso-velocity) contour distribution (Oxygen)

Case III: SOFC Fuel Cell

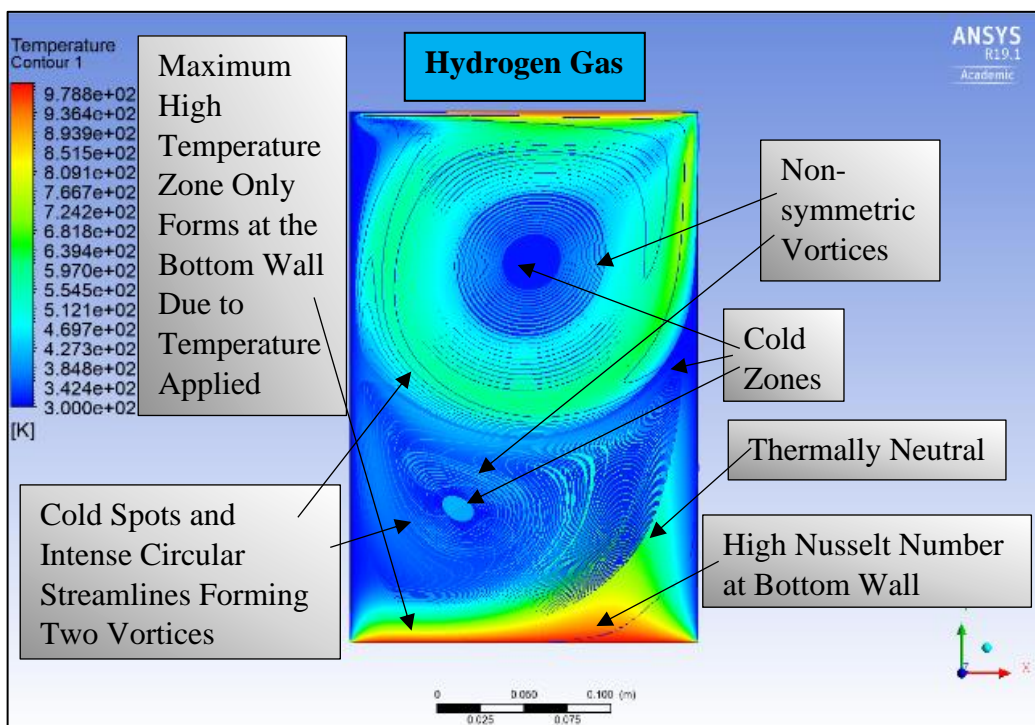


Figure 19a – Temperature contour distribution (Hydrogen)

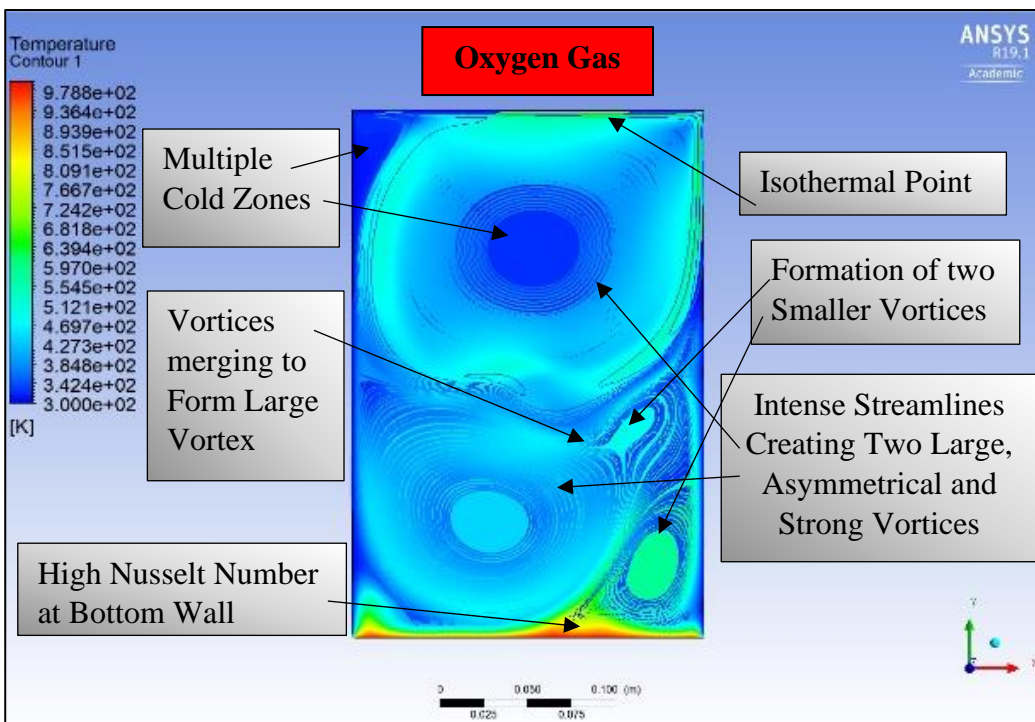


Figure 19b– Temperature contour distribution (Oxygen)

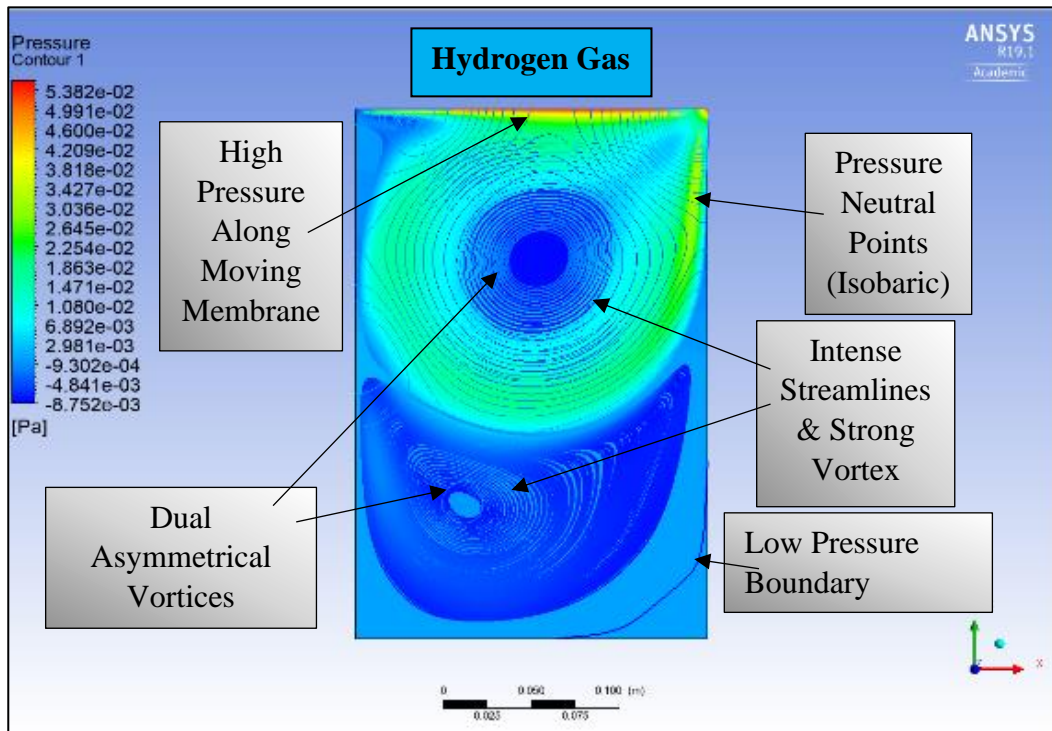


Figure 20a – Pressure contour distribution (Hydrogen)

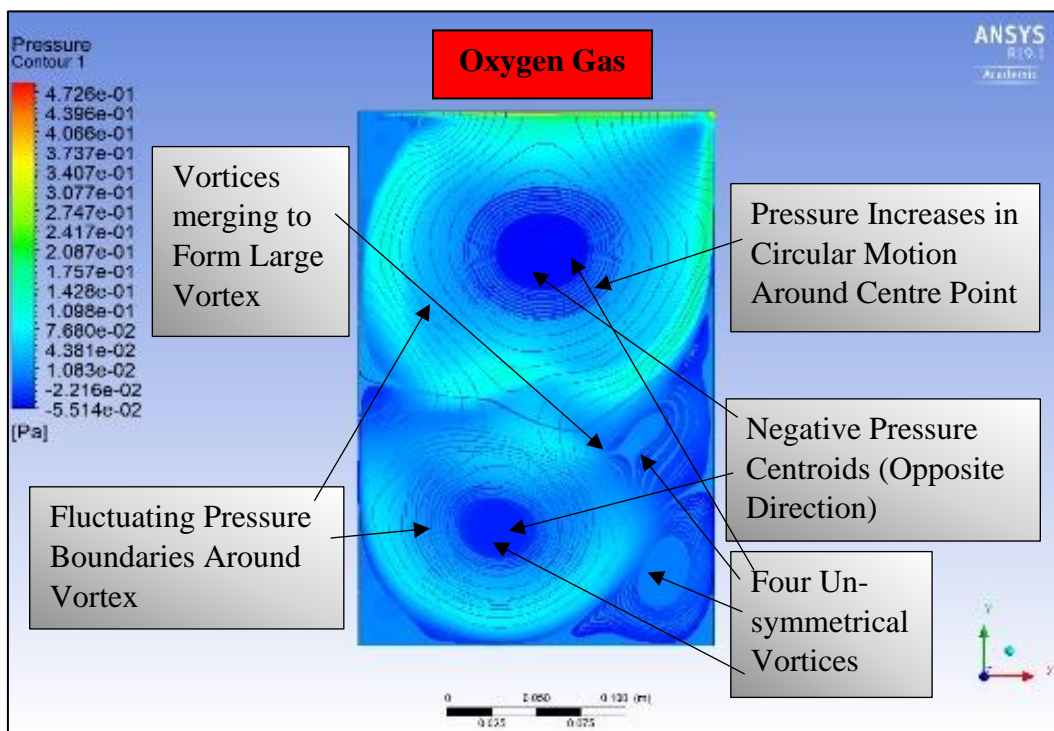


Figure 20b – Pressure contour distribution (Oxygen)

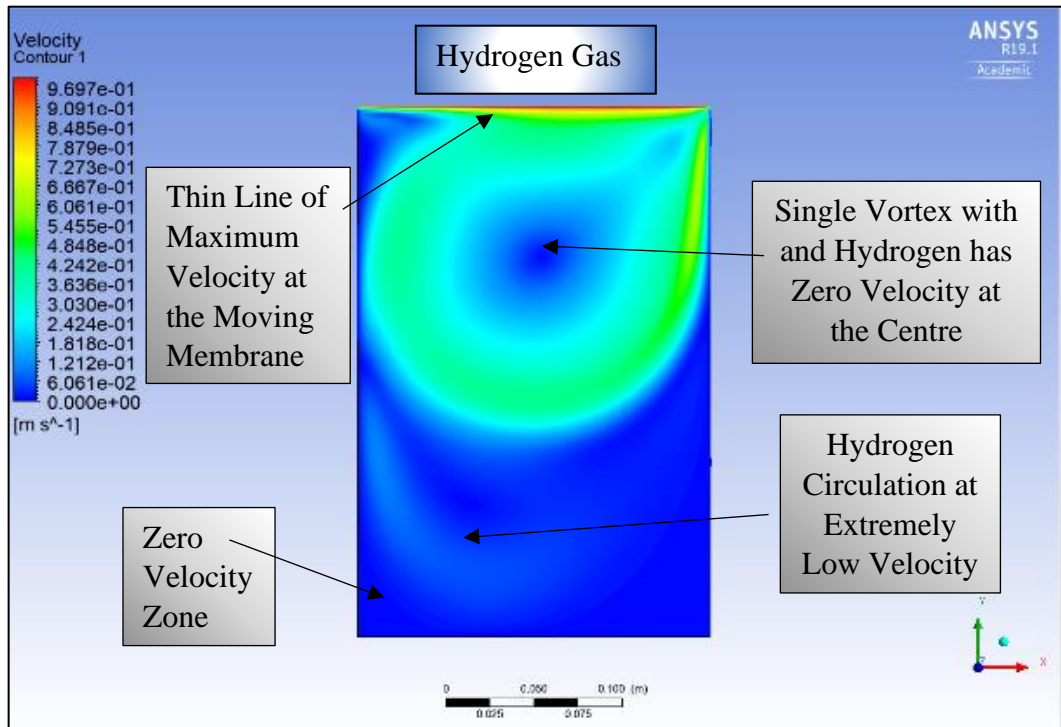


Figure 21a – Streamline (iso-velocity) contour distribution (Hydrogen)

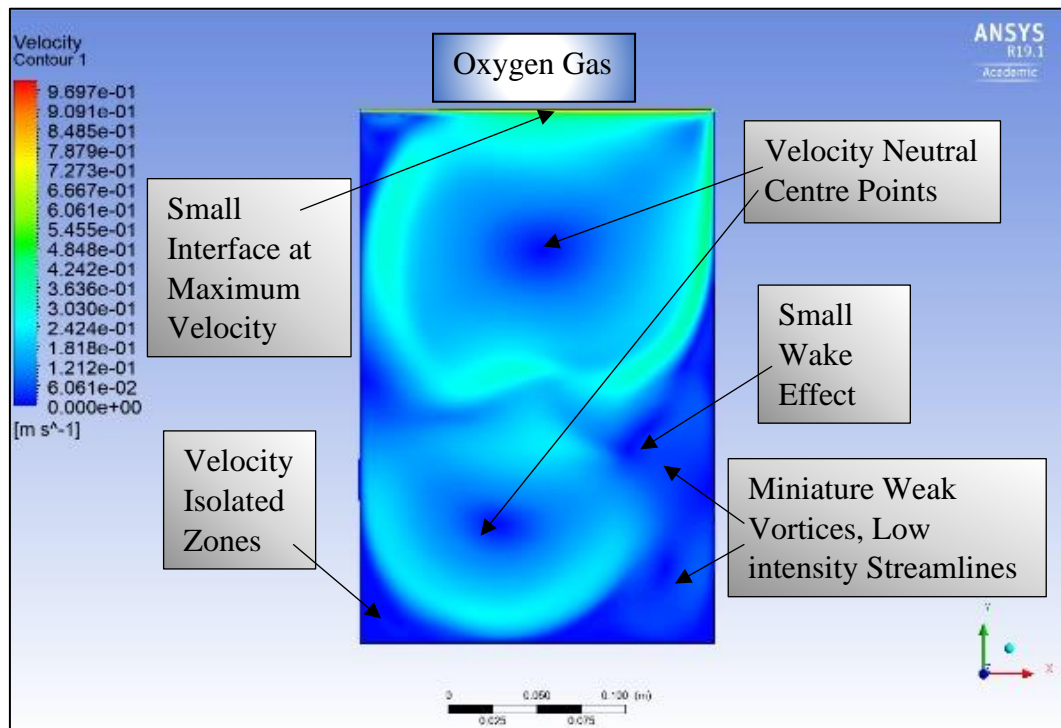


Figure 21b – Streamline (iso-velocity) contour distribution (Hydrogen)

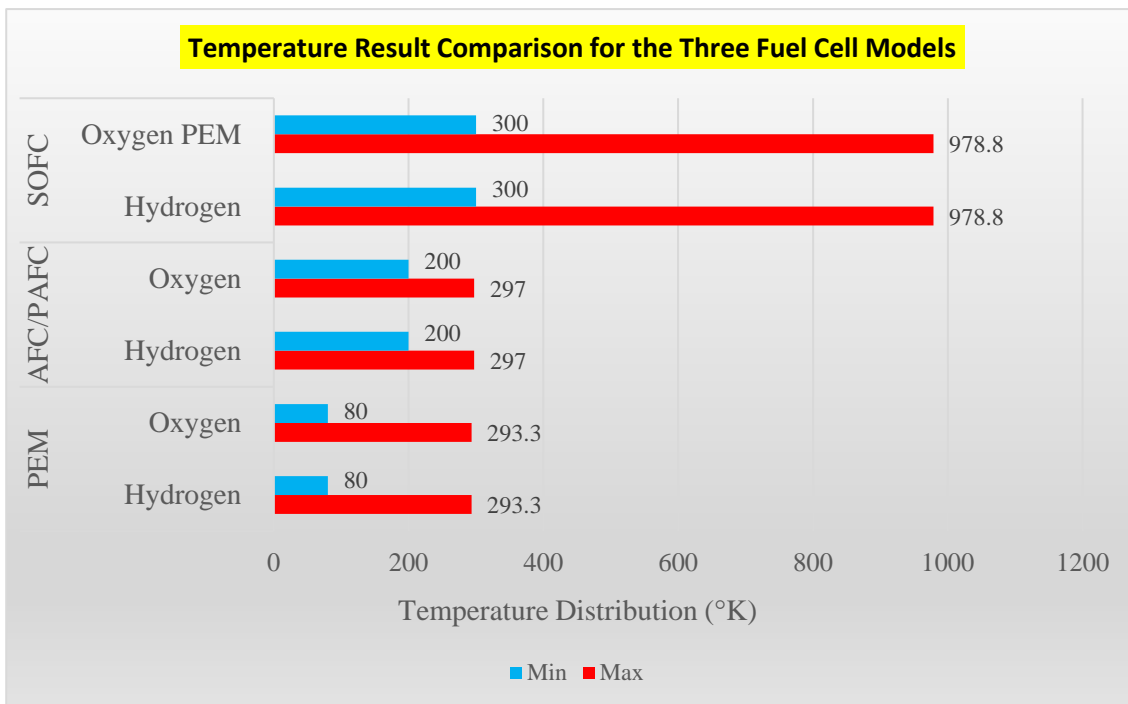


Figure 22 – Temperature Distribution Comparison Between all Three Models

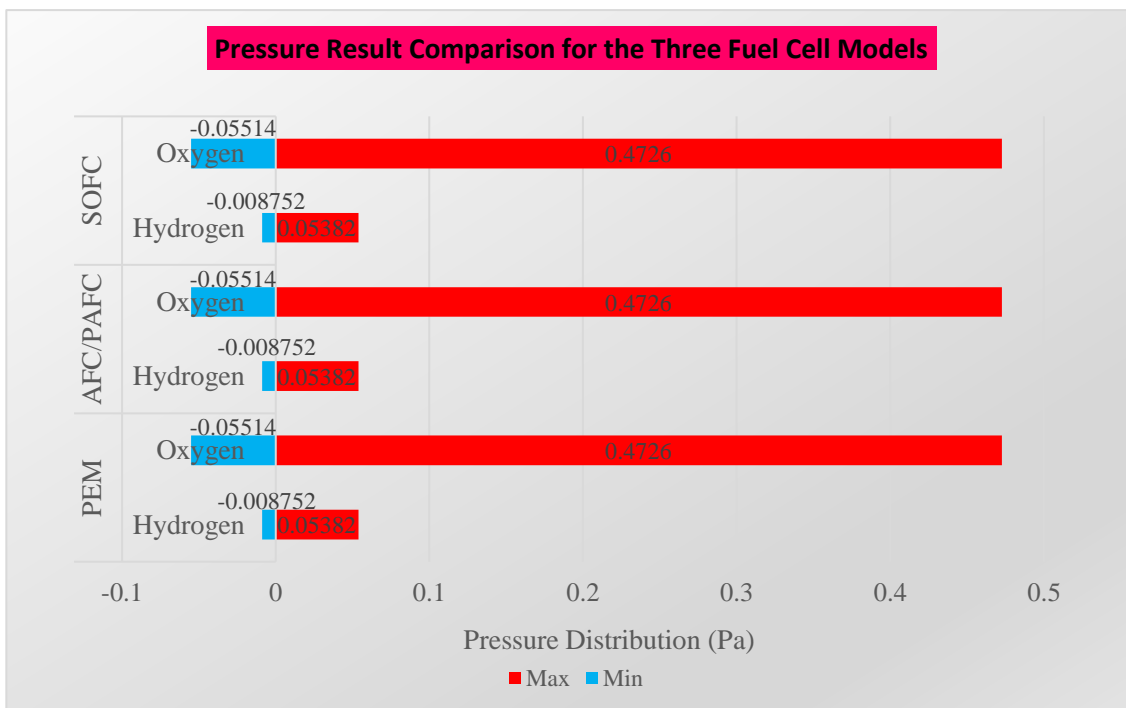


Figure 23 – Pressure Distribution Comparison Between all Three Models

Furthermore, **Figs. 22 and 23** summarize the temperature and pressure results for all three fuel cells. Implicit in the simulation have been the following model assumptions:

- i. The gases are not ideal.
- ii. The stack is fed with hydrogen and air.
- iii. The stack is equipped with a cooling system which maintains the temperature at the anode and cathode exits stable and equal to the stack temperature.
- iv. The stack is equipped with water management system ensuring the humidity within the cell is maintained at an appropriate level at any load.
- v. Pressure drops across flow channels is negligible.
- vi. Density does not vary.
- vii. The cell resistance is constant at any given condition of operation.
- viii. No radiation effects.
- ix. Prandtl number (ratio of momentum diffusivity to thermal diffusivity) is constant for each scenario.
- x. Wall temperatures (left, right and top are constant at room temperature).
- xi. Top wall has a velocity of 1ms^{-1} as it represents the moving membrane (Gas entry).
- xii. Rate at which the bottom wall temperature increases is constant (manually changed).
- xiii. Model is mesh dependent.
- xiv. Model is isotropic.

It is important to note that the distinctions between the fuel cells relate to the membrane material e.g. polymer, alkaline and solid oxide, not to the fuel gases which are either hydrogen or oxygen in all three sets of simulations considered.

Case I: PEM Fuel Cell

Figs. 13 a, b-15a, b illustrate the temperature, pressure and streamline contour plots for this first fuel cell type and for hydrogen fuel (a) and oxygen fuel (b). The temperature plots (**Figs. 13a,b**) for both hydrogen and oxygen gases show high temperatures at the wall implying a high mean high Nusselt number. The hydrogen temperature plot differs from the oxygen temperature plot shown since it exhibits only has two asymmetrical vortex structures whereas the oxygen plot generates four such vortices. Furthermore, the oxygen temperature plot shows one of the vortices merging with the lower vortex to form a larger vortex. The center points of the vortices for both plots show a relatively high temperature and intense low temperature zones surrounding the point itself. Commonly, the bottom wall of the membrane shows a cold zone, when both hydrogen and oxygen are inserted on the membrane platform. The maximum temperatures at the surrounding walls for either hydrogen or oxygen cases are $293.3\text{ }^{\circ}\text{K}$. The coldest areas within the membrane are at a temperature of 80°K . This is due to the convection that occurs between the gas and membrane body which leads to re-distribution of heat in the fuel cell enclosure. The pressure plots for the hydrogen and oxygen gases within the membrane are shown in **Figs. 14a, b**. A strong influence from thermal buoyancy force generates the formation of higher pressure in the opposite direction in the vicinity of the lower vortices (cells). Similar to the temperature plots the two vortices are again asymmetrical. There is a high-pressure zone shown at the top wall due to the moving membrane and high-pressure center points between the vortices in the opposite direction for both oxygen and hydrogen gas. The difference between the hydrogen and oxygen gas within the membrane is the formation of two small vortices when oxygen is used. Using hydrogen shows a single streamline at the bottom left chamfering the PEM fuel cell wall; however, this further develops when oxygen is used, and the intensity and volume of the streamlines increases, manifesting in the synthesis of two supplementary circulation zones i.e. cells. The pressure shown by one of the small vortices is substantially increasing and eventually merging with the large lower vortex is observed. The maximum pressure zones for when hydrogen and oxygen are inserted on the membrane are

5.382×10^{-2} and 4.73×10^{-1} Pa respectively. The low-pressure areas and neutral areas are shown in green and the negative pressures represent pressure in the opposite direction. Fig. 14a illustrates the lower base vortex with a pressure in the opposite direction at 8.75×10^{-3} Pa when hydrogen is inserted in the membrane. Fig. 14b shows the bottom vortex with a pressure in the opposite direction at 5.51×10^{-2} Pa when oxygen is inserted in the membrane. This is again intimately associated with the thermal buoyancy effect (relative to the viscous hydrodynamic force) which exacerbates thermal convection between the fuel gas and air in the membrane body. Finally, **Figs. 15 a, b** indicate that the streamline velocity plots exhibit the largest dissimilarity compared to the temperature and pressure plots when the gas changes from hydrogen to oxygen. When hydrogen is inserted on the membrane platform there is one vortex which forms at the top of the fuel cell membrane. The vortex has a velocity neutral center point and circulation is constrained with gas movement is limited at the upper region of the fuel cell. There is a high velocity zone at the moving membrane which is due to the applied velocity at the top wall of 1m/s i.e. the moving lid boundary condition. Therefore, the gas within the cell membrane platform has a low velocity relative to the top wall thus and progressively the gas circulates at velocities beneath 1 m/s. For the oxygen fuel case, within the PEM design, two vortices form, and the streamline intensity is relatively high, thus generating consistent gas circulation and spatially extensive low velocity zones. The streamlines merge to form a circulation pattern observed in both hydrogen and oxygen velocity plots. There is also a wake effect illustrated which arises due to the high velocity circulation around the upper vortex. The blue zones highlight velocity neutral zones and the gas is moving at 0 m/s at those points. Both Figs. show the high velocity zone at the moving membranes top wall with a velocity value of 0.9697 m/s. Even though the maximum velocity is 1 m/s the highest velocity measured of the gas movement is lower, which is due to frictional factors associated with viscous hydrodynamic forces.

Case II: AFC/PAFC Fuel Cell

Figs. 16 a, b visualize the temperature contour distributions for both hydrogen and oxygen fuel gas cases and it is apparent that high temperatures arise along the left wall, right wall and also top wall. The thermal distribution is therefore similar, to the PEM fuel cell setup at the fuel cell boundaries. The hydrogen temperature plot (Fig. 16a) differs from the oxygen temperature plot (Fig. 16b) mainly in that it exhibits only two asymmetrical vortices whereas the oxygen plot has four distinct circulation zones (vortices). Furthermore, the oxygen temperature plot shows one of the vortices merging with the lower vortex to form a larger vortex. The oxygen plot also shows a relatively large cold surface area however, the hydrogen plot shows relatively colder area by the dark blue zone shown by the lower vortex. The center points of the top vortices for both plots show a relatively high temperature and intense low temperature streamlines surrounding the point itself. Commonly, the bottom wall of the membrane shows a cold zone, when both hydrogen and oxygen are inserted on the membrane platform. The maximum temperatures at the surrounding walls for when hydrogen and oxygen are inserted on the membrane are 297 °K. The coldest areas within the membrane are at a temperature of 200°K. This is due to the convection that occurs between the gas and membrane body. In comparison to the PEM fuel cell there is approximately a 30% change in temperature whereas, the PEM cell shows a 60% temperature difference between the hot and cold zones. The pressure plots for the hydrogen and oxygen fuel gas cases are shown in **Figs. 17a, b**. Both reveal that higher pressure zones are synthesized in the opposite direction in the vicinity of the lower vortices. The two vortices which form are asymmetrical for both hydrogen and oxygen. There is a *high-pressure zone* shown at the top wall due to the moving membrane which is greater for the hydrogen model compared to the oxygen model. Furthermore, there are highly concentrated pressure points between the vortices in the opposite direction for both oxygen and hydrogen gas. The difference between the hydrogen and oxygen gas within the membrane is the formation of two small vortices when

oxygen is used, which is similar in the AFC/PAFC system geometry, but not identical to the PEM fuel cell model. The hydrogen model shows a single streamline at the bottom left chamfering the fuel cell surface however, it further develops when oxygen is used, and the intensity of the streamlines increases, producing two extra vortices. The pressure shown by one of the small vortices is substantially elevated and eventually there is a fusion with the large lower vortex. The maximum pressure zones for when hydrogen and oxygen computed on the membrane are 5.382×10^{-2} and 4.726×10^{-1} Pa respectively. The pressure neutral areas are shown in green and the negative pressures represent pressure in the opposite direction. Fig. 17a shows the bottom vortex with a pressure in the opposite direction at 8.75×10^{-3} Pa when hydrogen is inserted in the membrane. Fig. 17b shows the bottom vortex with a pressure in the opposite direction at 5.51×10^{-2} Pa when oxygen is inserted in the membrane. This is again connected to the relative influence of thermal buoyancy and viscous hydrodynamic force in the enclosure fuel cell regime. Finally, the streamline velocity plots (**Figs. 18a, b**) show the largest deviation computed when the gas changes from hydrogen to oxygen. However, the AFC model behaves generally similar to the PEM model. When hydrogen is inserted on the membrane platform there is a single vortex which forms at the top of the cell membrane. The vortex has a velocity neutral center point and circulation of increasing velocity which shows the gas movement is again confined principally to the upper region of the fuel cell. In addition, there is minimal hydrogen movement at speeds of 0.303 m/s at the bottom right of the membrane body. There is a high velocity zone at the moving membrane which was due to the applied velocity at the top wall of 1m/s, as it is a consistent design factor for all three models. Therefore, the gas within the cell membrane platform has a low velocity relative to the top wall thus and again can only achieve circulation at velocities of less than 1 m/s. When oxygen fuel is considered in the simulation, two circulation zones are generated and the streamline intensity is relatively high thus, forming consistent gas circulation in addition to low velocity zones. This behavior is again generally of a similar nature to that computed for the PEM model as the streamlines merge to form the circulation pattern shown in both hydrogen and oxygen iso-velocity plots. There is again high velocity and more vigorous circulation localized around the upper vortex. The blue zones highlight velocity neutral zones and the gas is moving at 0 m/s at those points. Both Figs.18a, b successfully capture the high velocity zone at the moving membranes top wall with a velocity value of 0.9697 m/s.

Case III: SOFC Fuel Cell

Unlike the PEM and AFC/PAFC models this model shows a variation in the temperature plots when both hydrogen and oxygen are used. The temperature plots for both hydrogen and oxygen gases exhibit higher magnitudes at the bottom wall where the temperature is applied. There is a markedly greater temperature at the base wall when hydrogen is applied as depicted in Fig. 19a in comparison to oxygen (Fig. 19b). This is probably attributable to the greater molecular weight of oxygen (atomic mass is sixteen times greater than hydrogen). The hydrogen model shows two large asymmetrical vortices. This differs to the oxygen model as the membrane shows a formation of four distinct but variable magnitude circulation zones (vortices). Furthermore, the oxygen temperature plot shows one of the vortices merging with the lower vortex to form a large vortex and in this regard the SOFC fuel cell performs similarly to the PEM and AFC/PAFC fuel cell models. The oxygen plot also shows a relatively large cold surface area however, the hydrogen plot shows relatively colder area by the dark blue zone associated with the lower vortex. The hydrogen plot shows multiple high temperature zones as demonstrated by the circulation at the top vortex. The center points of the top vortices for both plots show a relatively low temperature and intense high temperature (isotherms) surrounding the point itself. This trend is the opposite to that computed in the PEM and AFC fuel cell models. This is due to the substantially high temperature at the bottom wall. The plot shows relative temperature and since the base wall temperature is significantly high, the red zones are in the lower half of the fuel cell enclosure. Commonly, the base wall of the membrane [12-15] shows

a hot zone, when both hydrogen and oxygen are inserted on the membrane platform. The maximum temperatures at the base wall for both hydrogen and oxygen on the membrane are 978.8 °K. The coldest areas within the fuel cell are at a temperature of 300°K. The temperature difference throughout the SOFC model is approximately 60% which is similar to the PEM fuel cell model. The reason why the SOFC fuel cell works at such high temperatures is due to its application such as large appliances within large structures or powering larger hybrid vehicles and also other commercial systems (entire households). The pressure plots for the hydrogen and oxygen gases within the fuel cell are shown in **Figs. 20a, b** which again highlight that thermal buoyancy contributes substantially to the formation of higher pressure in the opposite direction at the base vortices. The two vortices which form are asymmetrical for both hydrogen and oxygen. There is a high-pressure zone shown at the top wall due to the moving membrane which is greater for the hydrogen model compared to the oxygen model. Furthermore, there are highly concentrated pressure points at the center of the vortices in the opposite direction for both oxygen and hydrogen gas. The difference between the hydrogen and oxygen gas within the membrane is the formation of two small vortices when oxygen is used, which is similar to both the PEM and AFC/PAFC fuel cell models. The hydrogen model shows a single streamline at the bottom left chamfering the membrane surface. This expands and further develops when oxygen is used, and the intensity and volume of the streamlines increases, leading to the formation of two extra vortices at the base half of the fuel cell. The pressure shown by one of the small vortices is substantially increasing thus, merging with the large lower vortex (Fig. 20a). The maximum pressure zones for when hydrogen and oxygen are inserted on the membrane are 5.382×10^{-2} and 4.726×10^{-1} Pa respectively which is the same as for the other two fuel cell models. The pressure neutral areas are shown in green and the negative pressures represent pressure in the opposite direction. Fig. 20a shows the base vortex with a pressure in the opposite direction at 8.75×10^{-3} Pa when hydrogen is inserted in the fuel cell. Fig. 20b shows the bottom vortex with a pressure in the opposite direction at 5.51×10^{-2} Pa when oxygen is inserted in the membrane. Again, thermal buoyancy is a strong contributor to this pattern and intensifies the interaction between the gas and air in the fuel cell. Finally, the streamline (iso-velocity) plots (**Figs. 21a, b**) exhibit significant disparity compared to the temperature and pressure plots when the fuel gas changes from hydrogen to oxygen. However, the overall behavior of the gas velocities is similar to the PEM and AFC/PAFC models. When hydrogen is inserted on the membrane platform there is one vortex which forms at the top of the cell membrane. The vortex has a velocity neutral center point and circulation with increasing velocity, indicating the gas movement is limited at the top of the cell. In addition, there is minimal hydrogen movement at speeds of 0.484 m/s at the bottom right of the membrane body. There is a high velocity zone at the moving membrane which is associated with the applied velocity at the top wall of 1m/s, as it is a consistent design factor for all three models. Therefore, the gas within the cell membrane platform has a low velocity relative to the top wall. Effectively once again, gas circulation is at speeds lower than 1 m/s. When oxygen is tested within the membrane, two vortices form, and the streamline intensity is relatively high thus, forming consistent gas circulation and larger but weaker velocity zones. This behavior is similar to the PEM model as the streamlines merge to form the circulation pattern shown in both hydrogen and oxygen velocity plots. The blue zones highlight velocity neutral zones and the gas is moving at 0 m/s at those points. Both streamline plots show the high velocity zone at the moving membranes top wall with a velocity value of 0.9697 m/s. There is also high velocity circulation around the upper vortex. The overall behavior of the gas velocities follows the same trend for all three fuel cell models, although there are distinct variations in selected zones for temperature (isotherm), pressure and streamline distributions and furthermore deviations are computed between the hydrogen and oxygen fuel cases. Good and efficient circulation and heat transfer is achieved in all three fuel cell configurations although further insight requires electrochemistry inclusion in the cathode/anode components which has been neglected in the current study.

5. FURTHER VALIDATION WITH THERMAL LBM CODE

Although mesh independence of the ANSYS FLUENT simulations has been conducted and described earlier, further corroboration of the accuracy of the finite volume computations requires an alternative numerical solution (in the absence of experimental verification). In this regard a *particle-based technique* is selected i.e. the Lattice Boltzmann method (LBM). This computational method is based on the microscopic particle models and mesoscopic kinetic equations. LBM builds simplified kinetic models that incorporate only the essential physics of microscopic or mesoscopic processes so that the macroscopic averaged properties obey the desired macroscopic equations. This subsequently avoids the use of the full Boltzmann equation, and avoids following each particle as in molecular dynamics simulations. Although LBM is based on a particle representation, the principal focus remains in the averaged macroscopic behaviour. The kinetic nature of the LBM introduces three important features that distinguish this methodology from other numerical methods. Firstly, the convection operator of the LBM in the velocity phase is linear. The inherent simple convection when combined with the collision operator allows the recovery of the nonlinear macroscopic advection through multiscale expansions. Secondly, the incompressible Navier–Stokes equations can be obtained in the nearly incompressible limit of the LBM. The pressure is calculated directly from the equation of state in contrast to satisfying Poisson's equation with velocity strains acting as sources. Thirdly, the LBM utilizes the minimum set of velocities in the phase space. Since only one or two speeds and a few moving directions are required, the transformation relating the microscopic distribution function and macroscopic quantities is greatly simplified and consists of simple arithmetic calculations. For thermal convection flows, the thermal LB model [23] is utilized which employs two distribution functions, f and g , for the flow and temperature fields, respectively. It was popularized by McNamara and Zanetti [24] who utilized it in their development of a multi-speed thermal fluid lattice Boltzmann method to solve heat transfer problems. Thermal LBM models the dynamics of fluid particles to capture macroscopic fluid quantities such as *velocity, pressure and temperature*. In this approach, the fluid domain is discretized to uniform Cartesian cells. Thermal LBM has been employed in several enclosure convection flows including Taoufik *et al.* [25, 26]. It has also been used in PEM fuel cell simulations [27-29]. The probability of finding particles within a certain range of velocities at a certain range of locations replaces tagging each particle as in the computationally intensive molecular dynamics simulation approach. In thermal LBM, each cell holds a fixed number of distribution functions, which represent the number of fluid particles moving in these discrete directions. The **D2Q9** model is very popular in this regard. The density and distribution functions i.e. f and g , are calculated by solving the Lattice Boltzmann equation (LBE), which is a special discretization of the *kinetic* Boltzmann equation. After introducing the BGK approximation, the general form of lattice Boltzmann equation with external force for a generalized enclosure thermal convection problem is:

For the flow field:

$$f_i(x + c_i \Delta t, t + \Delta t) = f_i(x, t) + \frac{\Delta t}{\tau_v} [f_i^{eq}(x, t) - f_i(x, t)] + \Delta t c_i F_k \quad (7)$$

For the temperature field:

$$g_i(x + c_i \Delta t, t + \Delta t) = g_i(x, t) + \frac{\Delta t}{\tau_c} [g_i^{eq}(x, t) - g_i(x, t)] \quad (8)$$

Here Δt denotes lattice time step, c_i is the discrete lattice velocity in direction i , F_k is the external force in direction of lattice velocity, τ_v and τ_c denotes the *lattice relaxation times* for the flow and temperature fields. The kinetic viscosity ν and the thermal diffusivity α , are defined in terms of their respective relaxation times, i.e. $\nu = c_s^2(\tau_v - 1/2)$ and $\alpha = c_s^2(\tau_c - 1/2)$, respectively. Note that the limitation $0.5 < \tau$ should be satisfied for both relaxation times to

ensure that viscosity and thermal diffusivity are positive. Furthermore, the *local equilibrium distribution function* determines the *type* of problem being simulated. It also models the equilibrium distribution functions, which are calculated with the following Eqns. for flow and temperature fields respectively:

$$f_i^{eq} = w_i \rho \left[1 + \frac{c_i \cdot u}{c_s^2} + \frac{1}{2} \frac{(c_i \cdot u)^2}{c_s^4} - \frac{1}{2} \frac{u^2}{c_s^2} \right] \quad (9)$$

$$g_i^{eq} = w_i T \left[1 + \frac{c_i \cdot u}{c_s^2} \right] \quad (10)$$

where w_i is a weighting factor and ρ is the lattice fluid (gas) density. For natural convection i.e. with thermal buoyancy, the Boussinesq approximation is applied.

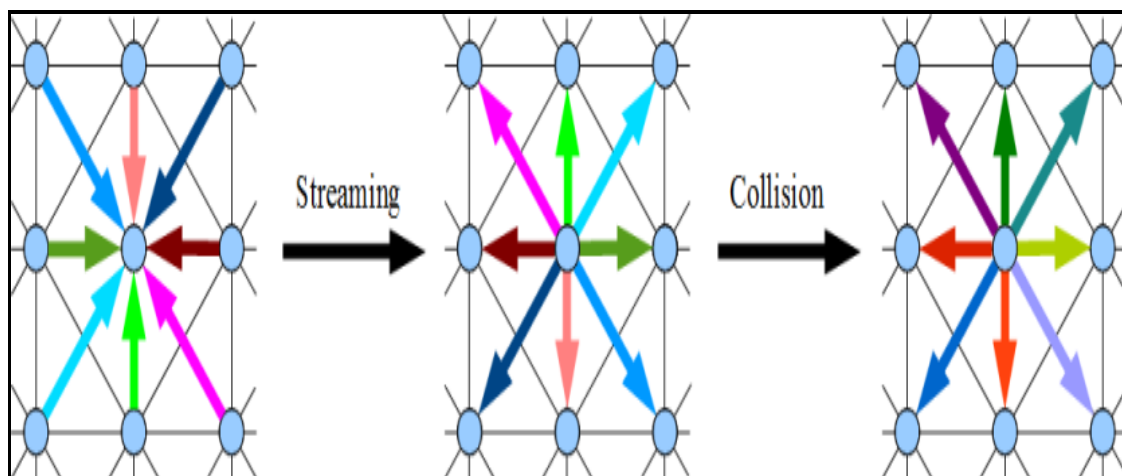


Fig 24: D2Q9 lattice in LBM

To ensure that the thermal LBM code works in the *near-incompressible regime*, the characteristic velocity of the flow for the natural convection regime ($V_{natural} \equiv \sqrt{\beta g_y \Delta TH}$) must be *small* compared with the fluid speed of sound. In most simulations, the characteristic velocity is adopted as 0.1 that of sonic speed. Bounce-back boundary conditions have to be applied on all solid boundaries, which indicate that incoming boundary populations are equal to out-going populations *after* the collision. Bounce back type boundary conditions are proven to provide more accurate numerical approximations for LBM simulations. Similarly, the temperature requires bounce back boundary condition (e.g. adiabatic) on different boundaries. A schematic of the **D2Q9 LBM** mesh is shown in **fig. 24**. Approximately 40,000 cells have been implemented to attain the desired accuracy after a cell independence test. Comparison has been conducted with several ANSYS FLUENT simulations (*Case 1: PEM fuel cell*, hydrogen gas i.e. **Figs. 13a and 15a**) as shown below. Excellent correlation has been attained. Compilation times were approximately 600-700s on an SGI Octane desk workstation. The comparisons are shown in **Figs. 25 and 26** for temperature and streamlines. Confidence in the ANSYS finite volume simulations is therefore justifiably very high.

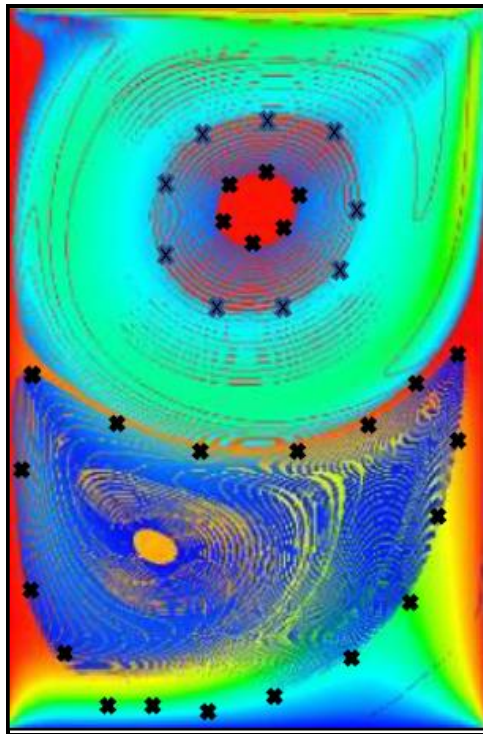


Fig. 25 ANSYS FLUENT versus Thermal LBM *temperature contours* (PEM hydrogen case) (N.B. crosses highlight LBM solution for outer periphery of selected circulation zones)

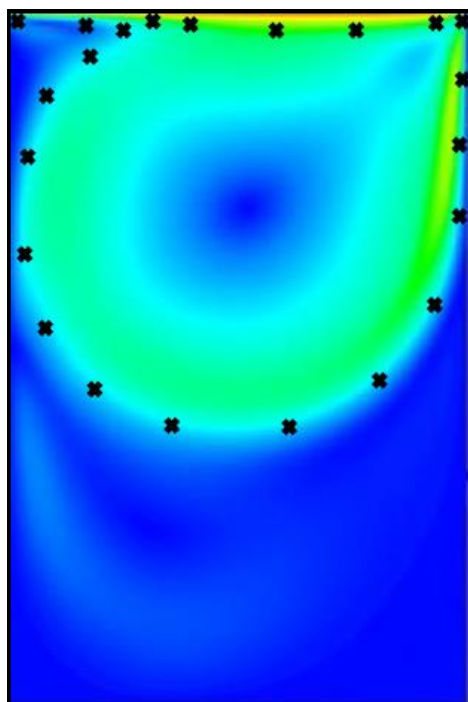


Fig. 26 ANSYS FLUENT versus Thermal LBM *streamline contours* (PEM hydrogen case) (N.B. crosses highlight LBM solution at outer periphery of selected circulation zone)

6. CONCLUSIONS

Detailed computational fluid dynamic simulation of simplified fuel cell systems are presented. ANSYS FLUENT finite volume commercial software (version 19) has been deployed to simulate flow characteristics and temperature distributions in a 2-dimensional enclosure replicating a hybrid hydrogen/oxygen fuel cell of the PEM, AFC/PAFC and SOFC type. Approximately 10,100 cells are used in the ANSYS simulations. Mesh independence tests are also performed. Extensive visualization of transport phenomena in the fuel cell is included i.e. streamline, pressure and isotherm contours. The top wall of the fuel cells was treated as a moving membrane which can relate to the entrance point of the gas and the bottom wall was heated which is treated as an external heat source. Validation of the finite volume computations has also been achieved with a thermal Lattice Boltzmann method (LBM) with a D2Q9 grid and 40,000 cells, achieving excellent agreement. The ANSYS simulations generally demonstrate that the overall behavior of the hydrogen or oxygen fuel gas velocities is similar in the PEM, AFC/PAFC and SOFC models. When hydrogen is inserted on the membrane platform there is one vortex which forms at the top of the cell membrane. The vortex has a velocity neutral center point and circulation with increasing velocity, indicating the gas movement is limited at the top of the cell. When oxygen is tested within the membrane, two vortices form, and the streamline intensity is relatively high thus, forming consistent gas circulation and larger but weaker velocity zones. There is also high velocity circulation around the upper vortex. The overall behavior of the gas velocities follows the same trend for all three fuel cell models, although there are distinct variations in selected zones for temperature (isotherm), pressure and streamline distributions and furthermore deviations are computed between the hydrogen and oxygen fuel cases. In the third configuration i.e. SOFC, the center points of the top vortices for both plots show a relatively low temperature and intense high temperature (isotherms) surrounding the point itself. This trend is contrary to that computed in the PEM and AFC fuel cell models. This is due to the substantially high temperature at the bottom wall. The current analysis has been confined to thermal convection within a simple rectangular geometry. Further studies will refine this geometry to consider serpentine channels, and also incorporate ANSYS FLUENT electrochemical reaction models [30] and will be reported imminently. Additionally, structural deformation can be explored to analyze the thermal stresses generated in individual fuel cell layers.

REFERENCES

- [1] Bhatt, S., Gupta, B., Sethi, V. K., & Pandey, M., Polymer Exchange Membrane (PEM) Fuel Cell: A Review. *International Journal of Current Engineering and Technology*, 2(1), 219-226 (2012).
- [2] Hamza Javaid, Investigating fuel cell technology in automobiles, *BEng (Hons) Mechanical Engineering, Final Year Project Report, Salford University, May (2019)*.
- [3] W. Vielstich, Arnold Lamm, Hubert A. Gasteiger, *Handbook of Fuel Cells: Fundamentals, Technology and Applications*, Wiley, New York (2003).
- [4] <https://www.toyota.co.uk/world-of-toyota/environment/fuel-cell-vehicle> (2020).
- [5] T.J. Chung, *Computational Fluid Dynamics*, CUP, New York (2002).
- [6] J.Macedo-Valencia *et al.*, 3D CFD modelling of a PEM fuel cell stack, *International Journal of Hydrogen Energy*, 41 (48) 23425-23433 (2016).
- [7] Awotwe, T. W., El-Hassan, Z., Khatib, F. N., Al Makky, A., Mooney, J., Barouaji, A., Olabi, A-G., Development of bi-polar plate design of PEM fuel cell using CFD techniques. *International Journal of Hydrogen Energy*, 42(40), 25663-25685 (2017).

- [8] S. Ravishankar, K. Arul and Prakash, Numerical studies on thermal performance of novel cooling plate designs in polymer electrolyte membrane fuel cell stacks, *Applied Thermal Engineering*, 66, 239-251 (2014).
- [9] X. Li *et al.* Molecular dynamics simulation study of a polynorbornene-based polymer: A prediction of proton exchange membrane design and performance, *16th China Hydrogen Energy Conference (CHEC 2015), November, Zhenjiang City, Jiangsu Province, China* (2015).
- [10] M. Nasri and Dave Dickinson, Thermal management of fuel cell-driven vehicles using HT-PEM and hydrogen storage, *9th International Conference on Ecological Vehicles and Renewable Energies (EVER)*, 25-27 March, Monte-Carlo, Monaco (2014).
- [11] A. Ranzo *et al.*, Validation of a three dimensional PEM fuel cell CFD model using local liquid water distributions measured with neutron imaging, *International Journal of Hydrogen Energy*, 39, 7089-7099 (2014).
- [12] Becker, J., Wieser, C., Fell, S., & Steiner, K., A multi-scale approach to material modelling of fuel cell diffusion media. *International Journal of Heat and Mass Transfer*, 54(7), 1360-1368 (2011).
- [13] Siegel, C., Review of computational heat and mass transfer modelling in polymer-electrolyte membrane (PEM) fuel cells. *Energy*, 33(9), 1331-1352 (2008).
- [14] Khan, M., Xiao, Y., Sundén, B., & Yuan, J., Analysis of multiphase transport phenomena in PEMFCs by incorporating microscopic model for catalyst layer structures, *Proc. 2011 ASME Int. Mech. Eng. Cong. and Exp., New York, IMECE2011-65142*, pp. 903912 (2011).
- [15] G. Mohan *et al.*, Analysis of flow maldistribution of fuel and oxidant in a PEMFC, *ASME J. Energy Resour. Technol*, 126(4): 262-270 (2004).
- [16] Y. Ding *et al.*, 3D simulations of the impact of two-phase flow on PEM fuel cell performance, *Chemical Engineering Science*, 100, 445-455 (2013).
- [17] J. Cao and N. Djilali, Numerical modeling of PEM fuel cells under partially hydrated membrane conditions, *ASME J. Energy Resour. Technol*, 127(1): 26-36 (2005).
- [18] G. Besagni *et al.*, Application of an integrated lumped parameter-CFD approach to evaluate the ejector-driven anode recirculation in a PEM fuel cell system, *Applied Thermal Engineering*, 121, 628-651 (2017).
- [19] J. Wang, Simulation of PEM fuel cells by OpenFOAM, *2014 MVK160 Heat and Mass Transport Conference, May 15, Lund, Sweden* (2014).
- [20] Y. Xiao, Dou, M., Yuan, J., Hou, M., Song, W., & Sundén, B. Fabrication process simulation of a PEM fuel cell catalyst layer and its microscopic structure characteristics. *Journal of The Electrochemical Society*, 159(3), B308-B314 (2012).
- [21] S. Chen and G.D. Doolen, Lattice Boltzmann method for fluid flows, *Ann. Rev. Fluid Mech.*, 30, 329-364 (1998).
- [22] O. Anwar Bég, T.A. Bég, H.J. Leonard, W.S. Jouri, A. Kadir, Electrochemical computation in hydrogen-based serpentine PEM fuel cells with ANSYS FLUENT, *Int. J Hydrogen Energy* (2020). *Submitted*
- [23] X. D. Niu, C. Shu, and Y. T. Chew, A thermal lattice Boltzmann model with diffuse scattering boundary condition for micro thermal flows, *Computers and Fluids*, 36, 273–281 (2007).
- [24] G.R. McNamara and G. Zanetti, Use of the Boltzmann equation to simulate lattice-gas automata, *Physical Review Lett.*, 61, 2332–2335 (1988).
- [25] Taoufik N, Jamil Z, Rajeb BM, Lattice Boltzmann analysis of 2-d natural convection flow and heat transfer within square enclosure including an isothermal hot block. *Int J Thermal Tech.*, 3:146-154 (2013).
- [26] Taoufik N, Ridha D., Natural convection flow and heat transfer in square enclosure asymmetrically heated from below: A lattice Boltzmann comprehensive study. *Computer Modelling in Engineering Sciences*, 88(3): 211-227 (2012).
- [27] L. Chen, Multi-scale modelling of proton exchange membrane fuel cell by coupling finite volume method and lattice Boltzmann method, *International Journal of Heat and Mass Transfer*, 63, 268-283 (2013).

- [28] B. Han and H. Meng, Numerical studies of interfacial phenomena in liquid water transport in polymer electrolyte membrane fuel cells using the lattice Boltzmann method, *International Journal of Hydrogen Energy*, 38, 5053-5059 (2013).
- [29] D. Froning and J. Liang, Impact of compression on gas transport in non-woven gas diffusion layers of high temperature polymer electrolyte fuel cells, *Journal of Power Sources*, 318, 26-34 (2016).
- [30] ANSYS FLUENT, *Theory Manual (fuel cells)*, Version 19, Lebanon, New Hampshire, USA (2019).